学位論文

Holographic Mean-Field Theory for QCD at Finite Density
（ホログラフィック平均場理論をもちいた有限密度 QCD の解析）

竹本　真平

Holographic Mean-Field Theory for QCD at Finite Density

Shinpei Takemoto

Department of physics, Nagoya University

March 2, 2012

abstract

QCD at finite temperature and/or density is one of the most important topics to study in hadron physics. The heavy-ion collision experiments in RHIC have shown signs of the phase transition from the hadronic phase to the quark-gluon plasma phase at high temperature regions. The superfluid state of the nuclear matter or the color superconducting state of the quark matter is expected to be realized at high density regions such as in neutron stars. The masses and the widths of hadrons are expected to vary at temperature and/or density due to the matter effect or the chiral symmetry restoration.

The main theme of this thesis is to obtain a holographic model which is applicable to QCD at finite baryon density. Most holographic models used to analyze finite-density systems do not include dynamical baryons. There are some attempts to include dynamical baryons into the model, but the dynamics of the baryons and that of the $U(1)_B$ gauge fields are not inclusively considered.

To resolve this problem, we propose a new mean-field approach, the holographic mean-field theory for fermion many-body systems. We introduce a non-vanishing classical fermionic field in the gravity dual, which we call the holographic mean field. The holographic mean field reflects the dynamics of the fermions in the bulk, and generates the expectation values of the bi-linear operators of the boundary fermions. This enables us to analyze finite-density systems of baryons in the confinement phase. Our method provides a new bulk condition which relates the chemical potential to the charge density in the GKP-Witten prescription. We apply our approach to a holographic model including dynamical baryons, which is originally proposed at zero density, and present the equation of state for baryon many-body systems.

Contents

Chapter 1

Introduction

Great efforts have been made to understand the dynamics of hadrons. Quantum Chromodynamics (QCD) is the fundamental theory which describes the strong interaction among quarks and gluons. QCD is a strong coupling gauge theory at the low energy region, which prevents us from solving the dynamics of hadrons analytically or perturbatively. This gives us a strong motivation to develop non-perturbative methods to analyze low energy physics of QCD, such as the first principle lattice QCD calculations or the effective model calculations.

Of these, the lattice QCD is a very powerful method, and it is used to calculate the hadron mass spectra [1] and the nuclear force [2]. The lattice QCD is also applied to analyze the finite-temperature system of hadrons, and the critical temperature at which the phase transition from the hadronic phase to the quark-gluon plasma phase occurs is estimated [3]. A disadvantage of the lattice QCD is that it suffers from the sign problem [4] at finite baryon density. There are some attempts to avoid this problem to analyze QCD at finite density [5], but it is still difficult to reveal the QCD phase diagram clearly. In this sense, QCD at finite density is an interesting subject in hadron physics.

Another method, the effective models are also widely used, and they sometimes provide deep insights about low energy physics of QCD. They suggest that QCD at finite density has plenty of interesting physical phenomena: At low temperature and high density region where quarks and gluons are deconfined, the color super conducting phase, where quarks form Cooper pairs may be realized [6]. This may affect cooling [7] or pulsar glitches [8] of neutron stars. At intermediate density such as in the nuclear matter, the masses or the decay widths of hadrons may change from those at vacuum [9]. This may affect the dilepton production rate observed in heavy-ion collision experiments [10]. However, we

have to keep in mind that the model results are not the results of QCD itself. Comparing the results obtained in various approaches is thus indispensable.

Recently, motivated by the gauge/gravity duality [11, 12, 13], there have been proposed some models to reformulate low energy QCD (a strong coupling gauge theory) in terms of a string theory (a weak coupling gravity theory). Such models are called the holographic QCD, and some of them successfully describe the meson mass spectra and the interactions among them [14, 15]. The holographic QCD is also applied to analyze QCD at finite temperature and/or density, while it is still developing.

In this thesis, we report our studies related to QCD at finite density:

In Chapter 2, we report our study on the QCD phase diagram using the Ginzburg-Landau theory. We pay a special attention to the possible existence of the phase where the bilinear quark (2-quark) condensate vanishes while the quartic quark (4-quark) condensate exists. We construct a chiral model which has the same chiral symmetry as in two-flavor QCD, $SU(2)_L \times SU(2)_R$, and allows unorthodox ($\to SU(2)_V \times (Z_2)_A$) as well as orthodox ($\to SU(2)_V$) pattern of chiral symmetry breaking. We study its phase diagram by applying one of the mean-field approaches, the Ginzburg-Landau theory. We also study the thermodynamic quantities and hadron mass spectra in the phases.

In Chapter 3, we review some previous studies about holographic models of QCD.

In Chapter 4, we report our study on the $\rho - a_1$ mixing in dense baryonic matter. We use a holographic model in the bottom-up approach and explore the dispersion relation of the $\rho - a_1$ mixture at finite baryon density taking into account the backreaction of the matter to the spacetime geometry.

Chapter 5 is the main part of this thesis. We propose a new mean-field approach, the holographic mean-field theory for QCD at finite baryon density. This approach enables us to analyze finite-density systems of baryons in the confinement phase. We apply our approach to a holographic model including dynamical baryons, which is originally proposed at zero density, and present the equation of state for baryon many-body systems.

We give a brief summary in Chapter 6.

Chapter 2

Thermodynamics with unbroken symmetry in two-flavor QCD

In this chapter, we report our study [16] on general features of thermodynamic quantities and hadron mass spectra in a possible phase, where the chiral $SU(2)_L \times SU(2)_R$ symmetry is spontaneously broken while its center Z_2 symmetry remains unbroken. We construct an $SU(2)_L \times SU(2)_R$ chiral model, which allows unorthodox ($\to SU(2)_V \times (Z_2)_A$) as well as orthodox ($\to SU(2)_V$) pattern of chiral symmetry breaking, and study its phase diagram by applying the Ginzburg-Landau theory.

2.1 Unorthodox pattern of chiral symmetry breaking

Chiral symmetry breaking plays an important role in acquiring hadron masses. The bilinear quark condensate $\langle\bar{q}q\rangle$ breaks chiral symmetry $SU(N_f)_L \times SU(N_f)_R$ down to the diagonal subgroup $SU(N_f)_V$. On the other hand, the quartic quark condensates

$$\langle O_1\rangle = \langle \bar{q}_L\lambda_a\gamma_\mu q_L \cdot \bar{q}_R\lambda_a\gamma^\mu q_R\rangle\,, \quad \langle O_2\rangle = \langle \bar{q}_R\lambda_a q_L \cdot \bar{q}_L\lambda_a q_R\rangle\,, \tag{2.1}$$
$$(\ \lambda_a\,(a = 1, 2, \cdots, N_f^2 - 1) \text{ are generators of } SU(N_f)\ )$$

break chiral symmetry down to $SU(N_f)_V \times (Z_{N_f})_A$ [17, 18, 19]. Although meson phenomenology with this breaking pattern seems to explain the reality reasonably [17], this possibility is strictly ruled out in QCD both at zero and finite

temperatures but at zero density since a different way of coupling of Nambu-Goldstone bosons to pseudo-scalar density violates QCD inequalities for density-density correlators [20]. However, this does not exclude the unorthodox pattern in the presence of dense baryonic matter. There are several attempts which dynamically generate a similar breaking pattern in an O(2) scalar model [21] and in $\mathcal{N} = 1$ Super Yang-Mills theory [22]. It is of particular interest to explore general features of thermodynamic quantities in the phase associated with this breaking pattern, which was not studied.

2.2 A model for 2-quark and 4-quark states

We construct a chiral Lagrangian for 2- and 4-quark states under the following pattern of symmetry breaking,

$$\begin{aligned} SU(N_f)_L \times SU(N_f)_R &\to SU(N_f)_V \times (Z_{N_f})_A \\ &\to SU(N_f)_V \,. \end{aligned} \tag{2.2}$$

In this study, we will restrict ourselves to a two-flavor case.

2.2.1 Lagrangian

We introduce a 2-quark state M in the fundamental and a 4-quark state Σ in the adjoint representation as [1]

$$\begin{aligned} M_{ij} &\sim \bar{q}_{R,j} q_{L,i} \,, \\ \Sigma_{ab} &\sim \bar{q}_L \tau_a \gamma_\mu q_L \bar{q}_R \tau_b \gamma^\mu q_R \,, \end{aligned} \tag{2.3}$$

where the flavor indices run $(i, j) = 1, 2$ and $(a, b, c) = 1, 2, 3$ and Pauli matrices $\tau^a = 2T^a$ with $\mathrm{tr}[T^a T^b] = \delta^{ab}/2$. The M and Σ are expressed as

$$\begin{aligned} M_{ij} &= \frac{1}{\sqrt{2}} \left(\sigma \delta_{ij} + i\phi^a \tau^a_{ij} \right) \,, \\ \Sigma_{ab} &= \frac{1}{\sqrt{3}} \chi \delta_{ab} + \frac{1}{\sqrt{2}} \epsilon_{abc} \psi_c \,, \end{aligned} \tag{2.4}$$

where σ and χ represent scalar fields and ϕ and ψ pseudoscalar fields, and ϵ_{ijk} is the total anti-symmetric tensor with $\epsilon_{123} = 1$. In general the field Σ contains an

[1] We consider Σ as any linear combination of $\bar{q}q$-$\bar{q}q$ and $\overline{qq}$-qq type fields allowed by symmetries.

isospin 2 state. One can take appropriate parameters in a Lagrangian in such a way that this exotic particle is very heavy. Thus, we will consider only isospin 0 (χ) and 1 (ψ) states in this study. The fields transform under $SU(2)_L \times SU(2)_R$ as

$$M \to g_L^{(2)} M g_R^{(2)\dagger}\,, \quad \Sigma \to g_L^{(3)} \Sigma g_R^{(3)\dagger}\,. \tag{2.5}$$

where $g_{L,R}^{(2)}$ is an element of $SU(2)_{L,R}$ in the fundamental representation, and $g_{L,R}^{(3)}$ in the adjoint representation. This transformation property implies that the field M changes its sign under the center Z_2 of $\mathrm{SU}(2)_L$ (or $\mathrm{SU}(2)_R$), while Σ is invariant:

$$M \to -M\,, \quad \Sigma \to \Sigma\,. \tag{2.6}$$

Up to the fourth order in fields one obtains a potential,

$$\begin{aligned} V(M,\Sigma) = & -\frac{m^2}{2}\mathrm{Tr}\left[MM^\dagger\right] + \frac{\lambda^2}{4}\left(\mathrm{Tr}\left[MM^\dagger\right]\right)^2 \\ & - \frac{\bar{m}^2}{2}\Sigma_{ab}\Sigma^T_{ba} + \frac{\bar{\lambda}_1^2}{4}\Sigma_{ab}\Sigma^T_{bc}\Sigma_{cd}\Sigma^T_{da} + \frac{\bar{\lambda}_2^2}{4}\left(\Sigma_{ab}\Sigma^T_{ba}\right)^2 \\ & + 2g_1\Sigma_{ab}\mathrm{Tr}\left[T_a M T_b M^\dagger\right] + g_2\Sigma_{ab}\Sigma^T_{ba}\mathrm{Tr}\left[MM^\dagger\right] \\ & + g_3\mathrm{Det}\Sigma + g_4(\mathrm{Det}M + \mathrm{h.c.})\,. \end{aligned} \tag{2.7}$$

The last term violates the $U(1)_A$ symmetry. The coefficients of the quartic terms are positive for this potential to be bounded. Other parameters g_i can be both positive and negative and will determine the topology of the phase structure. An explicit chiral symmetry breaking can be introduced through, e.g.,

$$V_{\mathrm{SB}}(M,\Sigma) = -h\sigma - \alpha h^2 \chi\,, \tag{2.8}$$

with constants h and α. Note that a similar Lagrangian was considered for a system with 2- and 4-quark states under the symmetry breaking pattern without unbroken center symmetry in [26] where their 4-quark states are chiral singlet and the potential does not include quartic terms in fields.

2.2.2 Ginzburg-Landau effective potential

We first study possible phases derived from the effective potential (2.7) taking [2]

$$M_{ij} = \frac{1}{\sqrt{2}}\sigma\delta_{ij}\,, \quad \Sigma_{ab} = \frac{1}{\sqrt{3}}\chi\delta_{ab}\,. \tag{2.9}$$

One can reduce Eq. (2.7) as well as an explicit breaking term to

$$\begin{aligned} V(\sigma,\chi) &= A\sigma^2 + B\chi^2 + \sigma^4 + \chi^4 - h\sigma \\ &\quad + C\sigma^2\chi + D\chi^3 + F\sigma^2\chi^2\,. \end{aligned} \tag{2.10}$$

We will take $C = -1$ without loss of generality in the following calculations.

We start with the potential for $D = F = 0$ and $h = 0$,

$$V = A\sigma^2 + B\chi^2 + \sigma^4 + \chi^4 - \sigma^2\chi\,. \tag{2.11}$$

Phases from this potential can be classified by the coefficients A and B. The expression of the phase boundaries is summarized in Appendix A. Here we discuss the obtained phase structure shown in Figure 2.1. There are three distinct phases characterized by two order parameters: Phase I represents the system where both chiral symmetry and its center are spontaneously broken due to non-vanishing expectation values χ_0 and σ_0. The center symmetry is restored when σ_0 becomes zero. However, chiral symmetry remains broken as long as one has non-vanishing χ_0, indicated by phase II. The chiral symmetry restoration takes place under $\chi_0 \to 0$ which corresponds to phase III. The phases II and III are separated by a second-order line, while the broken phase I from II or from III is by both first- and second-order lines. Accordingly, there exist two tricritical points (TCPs) and one triple point. One of these TCP, TCP_2 in Figure 2.1, is associated with the center Z_2 symmetry restoration rather than the chiral transition.

Two phase transitions are characterized by susceptibilities of the corresponding order parameters. We introduce a 2-by-2 matrix composed of the second derivatives of V as

$$\hat{C} = \begin{pmatrix} C_{\sigma\sigma} & C_{\sigma\chi} \\ C_{\chi\sigma} & C_{\chi\chi} \end{pmatrix}, \tag{2.12}$$

[2] The potential (2.7) does not exclude a possibility of $\langle\psi\rangle \neq 0$ leading to pion condensation. This corresponds to a further breaking of the symmetry down to $U(1)$. This is favored in a limited range of the parameters. In this study we will not consider this case but focus on the specific symmetry breaking pattern (2.2) and their consequences on the hadronic observables. The pion condensation is in fact unfavored when e.g. $\bar{\lambda}_1 = 0$ is taken.

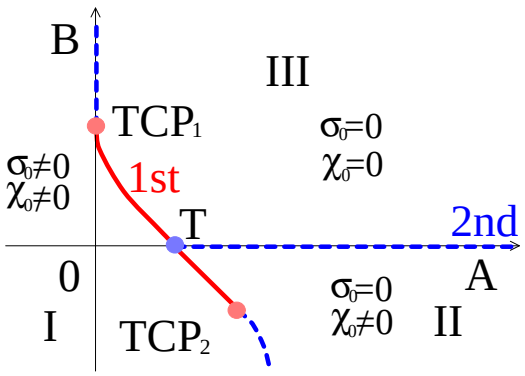

Figure 2.1: Phase diagram with $D = F = 0$ and $h = 0$. The solid and dashed lines indicate first and second order phase boundaries, respectively. One tricritical point, TCP_1, is located at $(A, B) = (0, 1/4)$ and another, TCP_2, at $(A, B) = (1/4, -1/8)$. The triple point represented by T is at $(A, B) = (1/8, 0)$.

with

$$C_{\sigma\sigma} = \frac{\partial^2 V}{\partial \sigma^2}\,, \quad C_{\chi\chi} = \frac{\partial^2 V}{\partial \chi^2}\,,$$
$$C_{\sigma\chi} = C_{\chi\sigma} = \frac{\partial^2 V}{\partial \sigma \partial \chi}\,, \tag{2.13}$$

under the solutions of the gap equations, σ_0 and χ_0. A set of susceptibilities is defined by the inverse of $\hat{C}$ [27];

$$\hat{\chi} = \frac{1}{\det \hat{C}} \begin{pmatrix} C_{\chi\chi} & -C_{\sigma\chi} \\ -C_{\chi\sigma} & C_{\sigma\sigma} \end{pmatrix}. \tag{2.14}$$

We identify the susceptibilities associated with 2-quark and 4-quark states as

$$\chi_{2\mathrm{Q}} = \hat{\chi}_{11}\,, \quad \chi_{4\mathrm{Q}} = \hat{\chi}_{22}\,. \tag{2.15}$$

The $\chi_{2\mathrm{Q}}$ is responsible to the Z_2 symmetry and the $\chi_{4\mathrm{Q}}$ to the chiral symmetry restoration.

We consider $\chi_{2\mathrm{Q}}$ and $\chi_{4\mathrm{Q}}$ around the TCP_1 in Figure 2.1 where the potential has zero curvature and thus $\det \hat{C} = 0$. When approaching the TCP_1 from broken phase I by tuning A and B as $A \to A_{\mathrm{critical}} = 0$ and $B = 1/4$, these susceptibilities diverge as

$$\chi_{2\mathrm{Q}} \sim t^{-1}\,, \quad \chi_{4\mathrm{Q}} \sim t^{-2/3}\,, \tag{2.16}$$

where $A_{\rm critical} - A \sim t$ with the reduced temperature or chemical potential, e.g. $t = |\mu - \mu_c|/\mu_c$. The gap equations determine the scaling of 2-quark and 4-quark condensates as

$$\sigma_0^2 \sim t^{1/3}\,, \quad \chi_0 \sim t^{1/3}\,. \tag{2.17}$$

Consequently, the quark number susceptibility $\chi_q = -\partial^2 V/\partial\mu^2$ exhibits a singularity as

$$\chi_q \sim \sigma_0^2 \cdot \chi_{\rm 2Q} \sim t^{-2/3}\,. \tag{2.18}$$

This critical exponent is same as the one in the 3-d Ising model. The coincidence can be understood due to the same Z_2 symmetries [3].

The critical behavior near the TCP_2 involves more: When the A is approached as $1/4 - t$ with $B = -1/8$ fixed, $\chi_{\rm 2Q}$ and $\chi_{\rm 4Q}$ diverge as

$$\chi_{\rm 2Q} \sim t^{-1}\,, \quad \chi_{\rm 4Q} \sim t^{-1/2}\,, \tag{2.19}$$

and only σ_0 vanishes as $\sigma_0^2 \sim t^{1/2}$. As a result, the quark number susceptibility χ_q diverges as

$$\chi_q \sim t^{-1/2}\,. \tag{2.20}$$

Note that the critical exponent $1/2$ is different from the one near the TCP_1, which may reflect different symmetries possessed by the system at TCP_2, $SU(2)_V$ and the center Z_2, from that at TCP_1, $SU(2)_L \times SU(2)_R$ including its center $(Z_2)_L \times (Z_2)_R$. Those exponents at $\mathrm{TCP}_{1,2}$ are changed when $D \neq 0$ (see below).

When the second-order phase transition separating phase I from II or from III is approached from the broken phase with a fixed B, we have

$$\chi_{\rm 2Q} \sim t^{-1}\,, \quad \chi_{\rm 4Q} \sim \frac{1}{B}\,, \tag{2.21}$$

where B is a finite number, which thus gives no singularities in $\chi_{\rm 4Q}$. The 2-quark condensate scales as $\sigma_0^2 \sim t^1$ and the quark number susceptibility χ_q is finite along the second-order phase transition line:

$$\chi_q \sim \sigma_0^2 \cdot \chi_{\rm 2Q} \sim t^0\,. \tag{2.22}$$

Nevertheless, χ_q is enhanced toward the phase transition induced by $\chi_{\rm 2Q}$ and becomes small above the phase transition. Such abrupt changes in χ_q indicate the

[3] The Z_2 symmetry in the 3-d Ising system is not the center of two-flavor chiral group, but emerges in the direction of a linear combination of quark number and scalar densities [28].

phase transition, especially for a negative B which is driven by the center symmetry restoration rather than the chiral phase transition.

Near the second-order chiral transition between phase II and III, one obtains from $B \sim t$

$$\chi_0^2 \sim t^1 , \quad \chi_{4Q} \sim t^{-1} . \tag{2.23}$$

Since chiral symmetry including the center symmetry prohibits the Yukawa-type coupling of χ to a fermion and an anti-fermion in the fundamental representation, the coupling of χ to the baryon number current would be highly suppressed. Therefore, χ_q shows less sensitivity around the chiral transition. [4]

Once small h is turned on, chiral symmetry and its center are explicitly broken. Second-order phase boundaries are replaced with cross over and the two TCPs with two critical points. The singularity in χ_q is now governed by the Z_2 universality class of 3-d Ising systems. Thus, the scaling of χ_q at the critical points (CPs) will be given by

$$\chi_q \sim t^{-2/3} . \tag{2.24}$$

A cubic term in χ modifies the previous phase structure shown in Figure 2.1. The phase diagram from the potential,

$$V = A\sigma^2 + B\chi^2 + \sigma^4 + \chi^4 - \sigma^2\chi + D\chi^3 , \tag{2.25}$$

is classified by the following regions of D: (i) $-1 < D < 0$, (ii) $D \leq -1$, (iii) $0 < D < 1$ and (iv) $1 \leq D$. One observes a deformation of the boundary lines depending on D as in Figure 2.2. The phase transition line separating phase II from phase III becomes of first order due to the presence of $D\chi^3$. For any negative D, (i) and (ii), a critical point CP_1 appears as a remnant of TCP_1 for $D = 0$. TCP_2 remains on the phase diagram for $-1 < D < 0$, (i), which eventually coincides with the triple point at $D = -1$, (ii). For positive D, (iii) and (iv), the transition line which separates phase I from phase II turns to be of first order everywhere. The triple point approaches the TCP_1 and coincides when a positive D reaches unity. The different order of phase transition between phase I and phase II for $-1 < D < 0$ to that for $0 < D < 1$ can be understood as follows: For $D = 0$ (see Figure2.1) the vacuum expectation value (VEV) χ_0 is positive in phase I near the phase boundary between phase I and II due to the existence of the $-\sigma^2\chi$ term in the potential. In phase II, on the other hand, when the positive χ_0 provides a local minimum of the potential, $-\chi_0$ also does, and both coincide with the global

[4] As we will show below, the phase transition from phase II to phase III is of first order in a more general parameter choice. Thus, χ_q exhibits a jump at the chiral phase transition point.

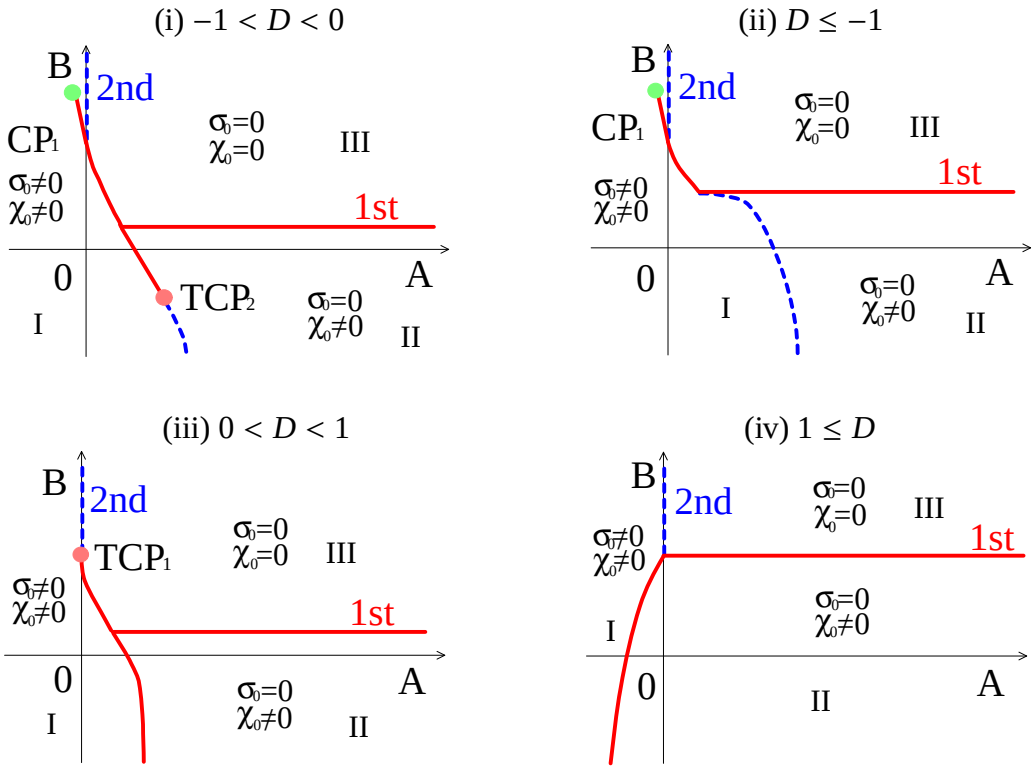

Figure 2.2: Phase diagram for different values of D under $F = 0$ and $h = 0$. The solid and dashed lines indicate first and second order phase boundaries, respectively.

	CP_1	TCP_1	TCP_2
$D < 0$	2/3	—	1/2
$D = 0$	—	2/3	1/2
$D > 0$	—	1/2	—

Table 2.1: The critical exponents of the quark number susceptibility for vanishing and non-vanishing D at two tricritical points and at the critical point (CP).

minima. These two vacua are physically equivalent, so that the phase transition from phase I to phase II can be of second order. When we add $D\chi^3$ term with negative D to the potential, the local minimum corresponding to the positive χ_0 is only the global minimum in phase II. This can be smoothly connected to the vacuum in phase I where the VEV χ_0 is positive. On the other hand, when D is positive, the negative χ_0 gives the global minimum in phase II. Thus, there is a mismatch of χ_0 along the phase boundary separating phase I from phase II, which indicates a first-order transition.

D also affects the quark number susceptibility χ_q. As in the case of $D = 0$, the χ_q exhibits a more relevant increase toward the Z_2 symmetry restoration than at the chiral phase transition. The critical exponents of χ_q is summarized in Table 2.1. One finds that the two regions, $D \leq 0$ and $0 < D$, corresponds to different universality. The cubic term plays a similar role to an explicit symmetry breaking term in the potential. This may be an origin for the appearance of a critical point.

For $-1 < D < 0$, TCP_2 for $h = 0$ becomes a critical point, CP_2, for finite h. When the value of h is increased, the CP_2 approaches the triple point and coincides with it for a certain value of h, h_0. The topology of the phase diagram for larger $h \geq h_0$ agrees with that for $D \leq -1$. Similarly, the TCP_1 in the $0 < D < 1$ phase diagram becomes a critical point CP_1 and disappears for a sufficiently large h. On the other hand, the CP_1 stays in the phase diagram Figure 2.2 (i) and (ii) for any value of h. The scaling of χ_q there will be given by

$$\chi_q \sim t^{-2/3} . \tag{2.26}$$

We note that adding finite F to the potential does not generate any essential differences from the above result with $F = 0$.

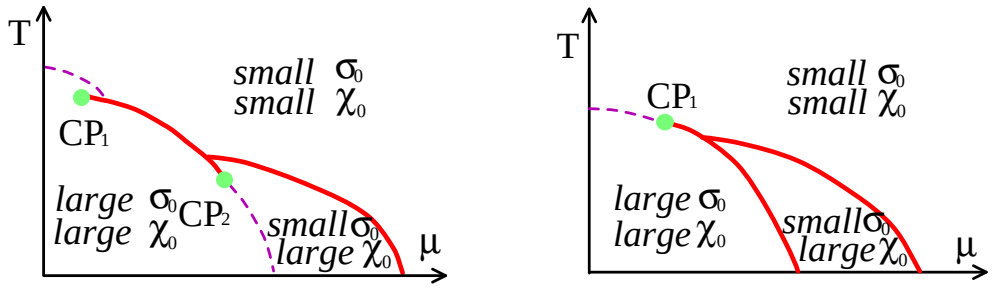

Figure 2.3: Schematic phase diagram mapped onto (T, μ) plane with a negative D (left) and with a positive D (right). The solid lines indicate first order phase boundaries, and dashed lines correspond to cross over.

2.3 Hypothetical phase diagram and quark number susceptibility

From the above observations one would expect phase diagrams mapped onto (T, μ) plane. In the chiral limit a new phase where the center symmetry is unbroken but chiral symmetry remains broken might appear in dense matter since at $\mu = 0$ this phase is strictly forbidden by the no-go theorem. With an explicit breaking of chiral symmetry one would draw a phase diagram as in Figure 2.3. The intermediate phase remains characterized by a small condensation $|\sigma_0| \ll |\chi_0|$. One would expect a new critical point associated with the restoration of the center symmetry, CP_2, rather than that of chiral symmetry if dynamics prefers a negative coefficient of the cubit term in χ. Multiple critical points in principle can be observed as singularities of the quark number susceptibility.

It has been suggested that a similar critical point in lower temperature could appear in the QCD phase diagram based on the two-flavored Nambu–Jona-Lasinio model with vector interaction [29] and a Ginzburg-Landau potential with the effect of axial anomaly [30]. There the interplay between the chiral (2-quark) condensate and BCS pairings plays an important role. In our framework without diquarks, the critical point discussed in Figure 2.3 (left) is driven by the interplay between the 2-quark and 4-quark condensates, and is associated with restoration of the center symmetry where anomalies have nothing to do with its appearance. Nevertheless, the cross over in low temperatures may have a close connection to the quark-hadron continuity [31] and it is an interesting issue to explore a possibility of

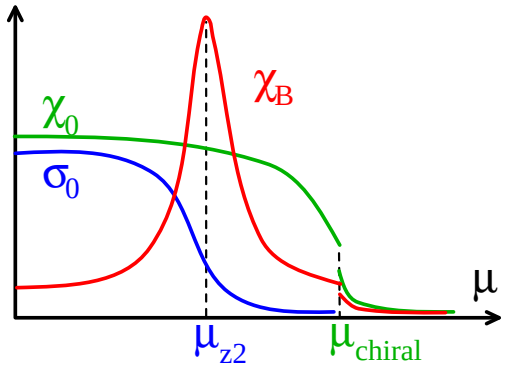

Figure 2.4: The behavior of the baryon number susceptibility as a function of chemical potential assuming the phase diagram of Figure 2.3 (left). The condensates and the susceptibility show a jump also at μ_{z2} when the phase structure of Figure 2.3 (right) is preferred.

dynamical center symmetry breaking in microscopic calculations. The present potential (2.10) leads to a first-oder transition of chiral symmetry even with an explicit breaking. This may be replaced with a cross over when one considers higher order terms in fields and other symmetry breaking terms as well as in-medium correlations to baryonic excitations, which is beyond the scope of this paper.

Appearance of the above intermediate phase seems to have a similarity to the notion of Quarkyonic Phase [24, 25], which is originally proposed as a phase of dense matter in large N_c limit. The transition from hadronic to quarkyonic world can be characterized by a rapid change in the net baryon number density. This feature is driven by the restoration of center symmetry and is due to the fact that the Yukawa coupling of χ to baryons is not allowed by the Z_2 invariance. Figure 2.4 shows an expected behavior of the quark (baryon) number susceptibility which exhibits a maximum when across the Z_2 cross over. This can be interpreted as the realization of the quarkyonic transition in $N_c = 3$ world. How far μ_{z2} from $\mu_{\rm chiral}$ is depends crucially on its dynamical-model description. [5]

It should be noticed that the critical point in low density region, indicated by

[5]Thus, the present analysis does not exclude the possibility that both transitions take place simultaneously and in such case enhancement of χ_B is driven by chiral phase transition. The phase with $\chi_0 \neq 0$ and $\sigma_0 = 0$ does not seem to appear in the large N_c limit [19, 20, 21]. It would be expected that including $1/N_c$ corrections induce a phase with unbroken center symmetry.

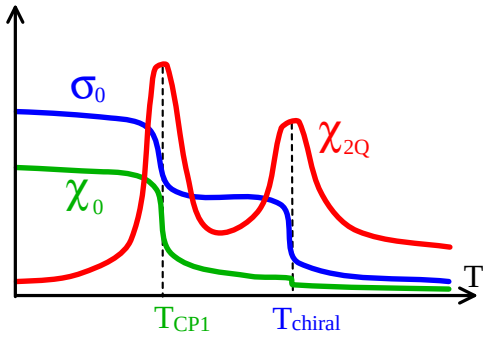

Figure 2.5: A schematic behavior of the susceptibility χ_{2Q} near the CP_1 as a function of temperature assuming the phase diagram of Figure 2.3 (left).

CP_1 in Figure 2.3 (left), is different from a usually considered CP [32] in the sense that the CP_1 is not on the cross over line attached to the $T = 0$ axis. When we take a path from the broken phase (both σ_0 and χ_0 are large) to the symmetric phase (both σ_0 and χ_0 are small) passing near the CP_1, the χ_{2Q} may exhibit two peaks; one is located near CP_1 and another is on the cross over line. We show a schematic behavior of χ_{2Q} as a function of temperature, together with σ_0 and χ_0 in Figure 2.5. The appearance of two peaks in χ_{2Q} reflects the fact that σ_0 becomes small across the CP_1 and the cross over. The first decrease in σ_0 near CP_1 is caused by a dropping of χ_0, while the second is by the chiral symmetry restoration.

2.4 Hadron mass spectra and pion decay constant

In this section we derive meson mass spectra in a linear sigma model. The Lagrangian with the potential (2.7) is expressed in terms of the mesonic fields as

$$\begin{aligned} \mathcal{L} &= \frac{1}{2}\left(\partial_\mu\sigma\partial^\mu\sigma + \partial_\mu\vec{\phi}\cdot\partial^\mu\vec{\phi}\right) \\ &+ \frac{1}{2}\left(\partial_\mu\chi\partial^\mu\chi + \partial_\mu\vec{\psi}\cdot\partial^\mu\vec{\psi}\right) - \mathcal{U}(\sigma,\phi,\chi,\psi)\,, \end{aligned} \tag{2.27}$$

with

$$\begin{aligned}\mathcal{U} &= -\frac{m^2}{2}\left(\sigma^2+\vec{\phi}^{\,2}\right)+\frac{\lambda^2}{4}\left(\sigma^2+\vec{\phi}^{\,2}\right)^2 \\ &-\frac{\bar{m}^2}{2}\left(\chi^2+\vec{\psi}^{\,2}\right)+\frac{\bar{\lambda}_1^2}{4}\left[\frac{1}{3}\chi^4+\frac{2}{3}\chi^2\vec{\psi}^{\,2}+\frac{1}{2}\left(\vec{\psi}^{\,2}\right)^2\right] \\ &+\frac{\bar{\lambda}_2^2}{4}\left(\chi^2+\vec{\psi}^{\,2}\right)^2-g\left[\frac{1}{2\sqrt{3}}\chi\left(3\sigma^2-\vec{\phi}^{\,2}\right)+\sqrt{2}\,\sigma\vec{\phi}\cdot\vec{\psi}\right] \\ &+\frac{g_3}{\sqrt{3}}\left(\frac{1}{3}\chi^3+\frac{1}{2}\chi\vec{\psi}^{\,2}\right), \end{aligned} \tag{2.28}$$

where $g_1 \equiv -g$ ($g > 0$) and $g_2 = 0$ were taken. In addition, we set $g_4 = 0$ since the g_4-term generates only a shift in m^2 for $N_f = 2$. We also set the explicit breaking being zero.

The condensate of the mesonic fields in the phase where both chiral symmetry and its center Z_2 are broken are determined from the coupled gap equations given by

$$\begin{aligned}\sigma_0^2 &= \frac{2}{\sqrt{3}\,g}\left(\frac{\bar{\lambda}^2}{3}\chi_0^2-\bar{m}^2+\frac{g_3}{\sqrt{3}}\chi_0\right)\chi_0\,, \\ \chi_0 &= \frac{1}{\sqrt{3}\,g}\left(\lambda^2\sigma_0^2-m^2\right), \end{aligned} \tag{2.29}$$

with $\bar{\lambda}^2 \equiv \bar{\lambda}_1^2 + 3\bar{\lambda}_2^2$. Shifting the fields as

$$\sigma \to \sigma+\sigma_0\,, \quad \chi \to \chi+\chi_0\,, \tag{2.30}$$

the potential reads

$$\begin{aligned}\mathcal{U} &= \frac{1}{2}m_\sigma^2\sigma^2+\frac{1}{2}m_\phi^2\vec{\phi}^{\,2}+\frac{1}{2}m_\chi^2\chi^2+\frac{1}{2}m_\psi^2\vec{\psi}^{\,2} \\ &\quad -\sqrt{3}\,g\sigma_0\,\sigma\chi-\sqrt{2}\,g\sigma_0\,\vec{\phi}\cdot\vec{\psi}+\cdots, \end{aligned} \tag{2.31}$$

where ellipses stand for the terms including the fields more than three, and

$$\begin{aligned}&m_\sigma^2 = 2\lambda^2\sigma_0^2\,, \quad m_\chi^2 = \frac{\sqrt{3}}{2}\frac{g}{\chi_0}\sigma_0^2+\frac{2}{3}\bar{\lambda}^2\chi_0^2+\frac{1}{\sqrt{3}}g_3\chi_0\,, \\ &m_\phi^2 = \frac{4}{\sqrt{3}}\,g\chi_0\,, \quad m_\psi^2 = \frac{\sqrt{3}}{2}\frac{g}{\chi_0}\sigma_0^2\,, \end{aligned} \tag{2.32}$$

The mass terms thus become

$$\begin{aligned}\mathcal{U}^{(2)} &= \frac{1}{2}(\sigma,\chi)\begin{pmatrix} m_\sigma^2 & -\sqrt{3}\,g\sigma_0 \\ -\sqrt{3}\,g\sigma_0 & m_\chi^2 \end{pmatrix}\begin{pmatrix}\sigma\\ \chi\end{pmatrix} \\ &+ \frac{1}{2}(\vec{\phi},\vec{\psi})\begin{pmatrix} m_\phi^2 & -\sqrt{2}\,g\sigma_0 \\ -\sqrt{2}\,g\sigma_0 & m_\psi^2 \end{pmatrix}\begin{pmatrix}\vec{\phi}\\ \vec{\psi}\end{pmatrix}. \end{aligned} \tag{2.33}$$

Obviously, the determinant of the above mass matrix for ϕ and ψ is zero and thus massless pseudo-scalar fields are a mixture of 2-quark and 4-quark states.

The mass eigenstates are introduced with a rotation matrix as

$$\begin{aligned}\begin{pmatrix} S \\ S' \end{pmatrix} &= \begin{pmatrix} \cos\theta & \sin\theta \\ -\sin\theta & \cos\theta \end{pmatrix}\begin{pmatrix}\sigma\\ \chi\end{pmatrix}, \\ \begin{pmatrix} \vec{P} \\ \vec{P}' \end{pmatrix} &= \begin{pmatrix} \cos\bar{\theta} & \sin\bar{\theta} \\ -\sin\bar{\theta} & \cos\bar{\theta} \end{pmatrix}\begin{pmatrix}\vec{\phi}\\ \vec{\psi}\end{pmatrix}, \end{aligned} \tag{2.34}$$

with the angles

$$\tan(2\theta) = \frac{2\sqrt{3}\,g\sigma_0}{m_\chi^2 - m_\sigma^2}, \quad \tan\left(2\bar{\theta}\right) = \frac{4\sqrt{6}\,\sigma_0\chi_0}{3\sigma_0^2 - 8\chi_0^2}. \tag{2.35}$$

The masses of scalar mesons are give by

$$\begin{aligned} m_S^2 &= m_\sigma^2\cos^2\theta + m_\chi^2\sin^2\theta - \sqrt{3}\,g\sigma_0\sin(2\theta), \\ m_{S'}^2 &= m_\chi^2\cos^2\theta + m_\sigma^2\sin^2\theta + \sqrt{3}\,g\sigma_0\sin(2\theta), \end{aligned} \tag{2.36}$$

and those of pseudo-scalar mesons by

$$m_P = 0, \quad m_{P'}^2 = \frac{g(3\sigma_0^2 + 8\chi_0^2)}{2\sqrt{3}\chi_0}, \tag{2.37}$$

with

$$\cos\bar{\theta} = \frac{\sqrt{3}\sigma_0}{\sqrt{3\sigma_0^2 + 8\chi_0^2}}, \quad \sin\bar{\theta} = \frac{2\sqrt{2}\chi_0}{\sqrt{3\sigma_0^2 + 8\chi_0^2}}. \tag{2.38}$$

The pion decay constant is read from the Noether current, $J_A^\mu \sim \sigma_0\partial^\mu\phi + 4/\sqrt{6}\,\chi_0\partial^\mu\psi$, as

$$F_\pi = \sqrt{\sigma_0^2 + \frac{8}{3}\chi_0^2}. \tag{2.39}$$

Since we consider a system in the chiral limit, the massive P' state is decoupled from the current and $F_{\pi'} = 0$, as it should be. It should be noted that, when $|\sigma_0| \gg |\chi_0|$, the NG boson is dominantly the 2-quark state. The 4-quark component becomes more relevant for $\sqrt{3}|\sigma_0| < \sqrt{8}|\chi_0|$, i.e. $\bar{\theta} > \pi/4$.

When the coupling g_3 is negative, which corresponds to $D < 0$ in the Ginzburg-Landau potential given in section 2.2, the phase transition from phase I ($\sigma_0 \neq 0$ and $\chi_0 \neq 0$) to phase II ($\sigma_0 = 0$ and $\chi_0 \neq 0$) can be of second order. In such a case, the restoration of the center Z_2 symmetry is characterized by vanishing σ_0. Approaching the restoration from broken phase, one finds the lowest scalar meson mass degenerate with the P state, while the pion decay constant remains finite due to $\chi_0 \neq 0$;

$$m_S \to m_P = 0\,, \quad F_\pi \to \sqrt{\frac{8}{3}}\chi_0\,, \tag{2.40}$$

with

$$\chi_0 = \sqrt{\frac{3\bar{m}^2}{\bar{\lambda}^2} + \left(\frac{\sqrt{3}\,g_3}{2\bar{\lambda}^2}\right)^2} - \frac{\sqrt{3}\,g_3}{2\bar{\lambda}^2}\,. \tag{2.41}$$

The vanishing S-state mass corresponds to a divergence of the susceptibility χ_{2Q}, which is responsible to restoration of the center symmetry. The scalar S and pseudo-scalar P states thus become the chiral partners on the phase boundary. In the Z_2 symmetric phase the meson masses are found from the potential (2.28) as

$$\begin{aligned} m_\sigma^2 &= -m^2 - \sqrt{3}\,g\chi_0\,, \quad m_\phi^2 = -m^2 + \frac{g}{\sqrt{3}}\chi_0\,, \\ m_\chi^2 &= \frac{2}{3}\bar{\lambda}^2\chi_0^2 + \frac{g_3}{\sqrt{3}}\chi_0\,, \quad m_\psi^2 = 0\,. \end{aligned} \tag{2.42}$$

There is no mixing in this phase, $\tan\theta = \tan\bar{\theta} = 0$, so that σ, ϕ, χ, ψ are the mass eigenstates. [6] This implies that the pure 4-quark state ψ is the massless NG boson in the Z_2 symmetric phase. Due to the broken chiral symmetry, σ and ϕ states are

[6] When we approach the phase boundary from the Z_2 symmetric phase to the Z_2 broken phase, m_σ^2 in Eq. (2.42) approaches zero, since $-m^2 = \sqrt{3}g\chi_0$ is satisfied at the phase boundary. The pseudoscalar mass m_ϕ^2 approaches $\frac{4}{\sqrt{3}}g\chi_0$ which coincides with the mass of P' in the Z_2 broken phase (see Eq. (2.37)).

not degenerate in mass. [7] The vector and axial-vector states neither degenerate in mass [20], since both vector and axial-vector currents are invariant under the Z_2 transformation but broken chiral symmetry does not dictate the same masses.

When $|g_3/g| \ll 1$, the chiral phase transition from phase II ($\sigma_0 = 0$ and $\chi_0 \neq 0$) to phase III ($\sigma_0 = 0$ and $\chi_0 = 0$) will be of weak first-order. In this case, χ_0 then F_π approach zero near the phase transition point. This is controlled by $\bar{m}$ approaching zero, which corresponds to B approaching zero in the Ginzburg-Landau potential discussed in section 2.2.2. The iso-spin 2 state will become very light near the phase transition. This may suggest that, when the $g_3\mathrm{Det}\Sigma$ term is small and the chiral phase transition is of weak first-order, a light exotic states with $I = 2$ might exist in dense baryonic matter. When there exists the non-negligible $g_3\mathrm{Det}\Sigma$ term, on the other hand, such state never becomes light since the chiral phase transition is of strong first-order.

In two flavors, the system would prefer the parity doubling for baryons in the Z_2 symmetric phase where the VEV χ_0 does not generate the baryon masses [20]. In the parity doubling scenario [33], all the baryons have their parity partners and then each pair of parity partners has a degenerate mass. On the other hand, in the naive scenario the lightest baryon does not have a parity partner, so that it becomes massless in the Z_2 symmetric phase. We list hadron mass spectra expected in phase I and phase II in Table 2.2.

2.5 Discussions

We have discussed a new phase where chiral symmetry is spontaneously broken while its center symmetry is restored. This might appear as an intermediate state between chirally broken and restored phases in (T, μ) plane. The appearance of the intermediate phase with unbroken Z_2 also suggests a new critical point associated with the center symmetry in low temperatures. A tendency of the center symmetry restoration is carried by the net baryon number density which shows a rapid increase and this is reminiscent of the quarkyonic transition. The $U(1)_A$ symmetry remains broken and the heavy η mass can be controlled with a certain anomaly coefficient.

[7] In reference [20] the degeneracy of the massive scalar and pseudoscalar mesons made of 4-quarks carrying the same isospin for a general number of flavors was shown. In case of $N_f = 2$ the $\mathrm{U}(1)_A$ anomaly generates a mass difference between the σ state and the pseudoscalar meson with $I = 0$ (η). In the present analysis, we did not include the $I = 0$ pseudoscalar and the $I = 1$ scalar mesons from the beginning by assuming that they are very heavy.

phase I: $\sigma_0 \neq 0, \chi_0 \neq 0$	phase II: $\sigma_0 = 0, \chi_0 \neq 0$
$SU(2)_V$	$SU(2)_V \times (Z_2)_A$
$m_S \neq 0, m_P = 0$ $m_V \neq m_A$	$m_S \neq m_P \neq 0, m_{P'} = 0$ $m_V \neq m_A$
$F_\pi = \sqrt{\sigma_0^2 + (8/3)\chi_0^2}$	$F_\pi = \sqrt{8/3}\chi_0$
$m_{N^+} \neq 0$	(i) naive: $\begin{cases} m_{N^+} = 0 \text{(ground state)} \\ m_{N'^+} = m_{N'^-} \neq 0 \\ \quad \text{(excited states)} \end{cases}$ (ii) mirror: $\begin{cases} m_{N^+} = m_{N^-} \neq 0 \\ \quad \text{(all states)} \end{cases}$

Table 2.2: The mass spectra of mesons and baryons in different phases for $N_f = 2$. Baryons transform with the naive chirality assignment as $\psi_{R,L} \to g_{R,L}\psi_{R,L}$, while with the mirror assignment as $\psi_{1R,L} \to g_{R,L}\psi_{1R,L}$ and $\psi_{2R,L} \to g_{L,R}\psi_{2R,L}$ with $g_{R,L} \in SU(2)_{R,L}$ where two nucleons ψ_1 and ψ_2 belong to the same chiral multiplets.

There are subtleties in baryon masses since the existence of the center symmetry does not immediately dictate the parity doubling for a general number of flavors: Here we consider the case in massless three flavors. The g_3-term in (2.7) now generates χ^8 contribution, while the g_4-term does σ^3 one. It follows that $D\chi^3$ is removed from (2.10) and another cubic term σ^3 is added. Omitting the cubic term σ^3 results in the same phase diagram as Figure 2.1 with two TCPs. When the cubic term σ^3 is included, it is conceivable that phase II and phase III in Figure2.2 are separated by a second-order phase boundary, which will become a first-order one when we take quantum fluctuations into account [34]. The topologies are expected to be quite similar to those shown in Figure 2.2, so that we expect a strong enhancement of the quark number susceptibility at the Z_3 restoration point. Differently from the case for $N_f = 2$, the Σ_{ab} field is allowed to couple to the octet baryon states as, e.g. $\bar{B}_a\Sigma_{ab}B_b$, and the baryon number current couples to the χ state which becomes massless at the chiral restoration point. As a result, the quark number susceptibility might show another peak at the chiral restoration. Hadron masses in the Z_3 symmetric phase are slightly different from those under Z_2 invariance: In the mesonic sector the party partners are degenerate and the degeneracy does not generally occur in the baryonic sector [20]. Following Ref. [20], possible

phase I: $\sigma_0 \neq 0\,, \chi_0 \neq 0$	phase II: $\sigma_0 = 0\,, \chi_0 \neq 0$
$SU(N_f)_V$	$SU(N_f)_V \times (Z_{N_f})_A$
$m_S \neq 0\,, m_P = 0$ $m_V \neq m_A$	$m_S = m_P \neq 0,\, m_{P'} = 0$ $m_V \neq m_A$
$m_{N^+} \neq 0$	(i) naive: $m_{N^+} \neq 0$ (ii) mirror: $m_{N^+} = m_{N^-} \neq 0$

Table 2.3: Same as in Table 2.2 but for $N_f = 3$.

operators for the baryons are expressed as

$$\begin{aligned} B_L^1 &= (q_L q_L q_R)_L\,,\ B_L^2 = (q_L q_R q_R)_L\,,\ B_L^3 = (q_L q_L q_L)_L\,, \\ B_R^1 &= (q_R q_R q_L)_R\,,\ B_R^2 = (q_R q_L q_L)_R\,,\ B_R^3 = (q_R q_R q_R)_R\,, \end{aligned} \tag{2.43}$$

where the color and flavor indices are omitted. For the octet baryons, the representations under the chiral SU(3)$_L$×SU(3)$_R$ of these baryonic fields are assigned as

$$\begin{aligned} &B_L^1 \sim (\bar{3}\,,\, 3)\,, \quad B_L^2 \sim (3\,,\, \bar{3})\,, \quad B_L^3 \sim (8\,,\, 1)\,, \\ &B_R^1 \sim (3\,,\, \bar{3})\,, \quad B_R^2 \sim (\bar{3}\,,\, 3)\,, \quad B_R^3 \sim (1\,,\, 8)\,. \end{aligned} \tag{2.44}$$

When the B^3 is the lightest octet baryon, which we call the naive assignment, it is still massive in the Z_3 symmetric phase, since the Yukawa coupling of the 4-quark state Σ_{ab} is possible as, e.g. $\bar{B}_a \Sigma_{ab} B_b$. When the lightest baryons are described by a combination of B^1 and B^2, which we call the mirror assignment, they are degenerate with each other in the Z_3 symmetric phase. We summarize these features in Table 2.3. The baryon masses crucially depend on a way of chirality assignment. It would be an interesting issue to clarify this within a more elaborated model.

The main assumption in this study is a dynamical breaking of chiral symmetry $SU(N_f)_L \times SU(N_f)_R$ down to a non-standard $SU(N_f)_V \times (Z_{N_f})_A$ although this seems to be theoretically self-consistent. Calculations using the Swinger-Dyson equations or Nambu–Jona-Lasinio type models with careful treatment of the quartic operators may directly evaluate this reliability. Besides, anomalously light NG bosons, $m_\pi^2 \sim O(m_q^2)$, could lead to an s-wave pion condensation as discussed in [35]. It is interesting to explore how this phase is embedded in the

current analysis. A calculation using the Skyrme model shows a similar intermediate phase [23]. Although the above non-standard pattern of symmetry breaking was not imposed in the Skyrme Lagrangian, the result could suggest an emergent symmetry in dense medium. This intermediate phase would be an intriguing candidate of the quarkyonic phase if it could sustain in actual QCD at finite density and would lead to a new landscape of dense baryonic matter.

Chapter 3

Holographic models of QCD

In this chapter, we review some holographic models of QCD. There are two complementary approaches in holographic QCD — the bottom-up approach and the top-down approach. In the bottom-up approach, we start from QCD and attempt to construct its 5d holographic dual by using the AdS/CFT dictionary. The benefit of the bottom-up approach is that it is easier to bring in phenomenological aspects of QCD. In Section 3.1, we review one of the bottom-up models, the hard wall model [15]. In the top-down approach, we engineer a brane configuration in string theory so as to make its holographic dual closer to QCD. The top-down approach is more faithful to the AdS/CFT correspondence, and thus more reliable. In Section 3.2, we review one of the top-down models, the Sakai-Sugimoto model (SS model) [14]. The SS model successfully describes low energy properties of QCD, especially the meson phenomenology. In Section 3.3, we review some attempts to introduce baryons into the SS model.

3.1 The hard wall model

We construct a 5d dual of QCD in AdS_5 space, whose metric is given by

$$ds^2 = \frac{1}{z^2}(-dz^2 + dx^\mu dx_\mu)\,, \tag{3.1}$$

where we set the AdS radius to unity. We set a UV boundary at $z = \epsilon \sim 0$, where a 4d theory, QCD lives, and an IR cutoff at $z = z_m$, which corresponds to the confining scale. Thus, the fifth direction is restricted to

$$\epsilon \leq z \leq z_m\,. \tag{3.2}$$

4d (Operator)	5d (Field)	$(m_5)^2$
$\bar{q}_L \gamma^\mu t^a q_L$	$A^a_{L\mu}$	0
$\bar{q}_R \gamma^\mu t^a q_R$	$A^a_{R\mu}$	0
$\bar{q}^\alpha_R q^\beta_L$	$(2/z)\, X^{\alpha\beta}$	-3

Table 3.1: Operators/Fields of the model.

This model is called the hard wall model, which is most widely used in the bottom-up approach. In the bottom-up approach, we introduce a few bulk 5d fields corresponding to 4d operators. As an example, we choose three fields $A^a_{L\mu}, A^a_{R\mu}$ and X listed in Table 3.1.

The 5d mass m_5 of the fields are determined by the relation [12, 13] $(\Delta - p)(\Delta + p - 4) = m_5^2$, where Δ and p denote the dimension and the spin of the corresponding operator, respectively. The 5d action is given by

$$S = \int d^4x dz \sqrt{g}\, \mathrm{tr}\left[|DX|^2 + 3|X|^2 - \frac{1}{4g_5^2}(F_L^2 + F_R^2) \right], \tag{3.3}$$

where $D_\mu X = \partial_\mu X - iA_{L\mu}X + iXA_{R\mu}$, $A_{L,R} = A^a_{L\mu} t^a$ and $F_{\mu\nu} = \partial_\mu A_\nu - \partial_\nu A_\mu - i[A_\mu, A_\nu]$. This action is $SU(N_f)_L \times SU(N_f)_R$ gauge invariant, which corresponds to the global chiral symmetry in QCD.

Since the bulk field X corresponds to the 4d operator $\bar{q}q$, its behavior describes chiral symmetry breaking in this model. We perform the mean-field approximation for $X(x, z)$ by replacing it with the mean field $X_0(z)$ as

$$X(x, z) \to X_0(z)\,. \tag{3.4}$$

We impose that $(2/z)\, X_0(z)$ coincides with the quark mass matrix M at the UV boundary as

$$\frac{2}{\epsilon} X_0(\epsilon) = M\,. \tag{3.5}$$

The equation of motion for $X_0(z)$ is

$$\left[\partial_z \left(\frac{1}{z^3} \partial_z \right) + \frac{3}{z^5} \right] X_0(z) = 0\,, \tag{3.6}$$

and its solution is written as

$$X_0(z) = \frac{1}{2} Mz + \frac{1}{2} \Sigma z^3\,. \tag{3.7}$$

By substituting the equation of motion, the on-shell action for X becomes

$$S_X = \int d^4x \left(\frac{1}{z^3} X_0(z)\, \partial_z X_0(z) \right)_{z=\epsilon} . \tag{3.8}$$

Differentiating this with respect to M, we obtain

$$\left. \frac{\delta S_X}{\delta M} \right|_{M=0, z=\epsilon} = \Sigma , \tag{3.9}$$

which tells us to interpret Σ as the chiral condensate: $\Sigma^{\alpha\beta} = \langle \bar{q}^\alpha q^\beta \rangle$. Σ is determined by the IR condition on X. Instead of specifying this condition, we choose Σ as an input parameter of the model. We assume that the quark masses are degenerated, $M = m_q \mathbf{1}$ and $\Sigma = \sigma \mathbf{1}$. Therefore, the free parameters of the model are m_q, σ, z_m and g_5. We focus on the two-flavor case and use the experimental values of the ρ meson mas, the pion mass and the pion decay constant to fix m_q, σ, z_m.

The 5d gauge coupling g_5 is fixed by comparing the vector current two-point function in this model with that of QCD. We introduce the vector field V as

$$V = \frac{A_L + A_R}{2} . \tag{3.10}$$

In the $V_z = 0$ gauge, the equation of motion for the transverse part of the vector field is

$$\left[\partial_z \left(\frac{1}{z}\, \partial_z \right) + \frac{q^2}{z} \right] V_\mu^a(q, z) = 0 , \tag{3.11}$$

where $V_\mu^a(q, z)$ is the 4d Fourier transform of $V_\mu^a(x, z)$. The on-shell action for the vector field is

$$S_V = -\frac{1}{2g_5^2} \int d^4x \left(\frac{1}{z} V_\mu^a \partial_z V^{\mu a} \right)_{z=\epsilon} . \tag{3.12}$$

Let $V_{0\mu}^a(q)$ be the Fourier transform of the source of the vector current $J_\mu^a = \bar{q} \gamma_\mu t^a q$. We impose

$$V_\mu^a(q, \epsilon) = V_{0\mu}^a(q) , \tag{3.13}$$

thus $V(q, z)$, which is defined as

$$V_\mu^a(q, z) = V(q, z) V_{0\mu}^a(q) , \tag{3.14}$$

is required to satisfy

$$V(q, \epsilon) = 1 . \tag{3.15}$$

Differentiating the on-shell action twice with respect to the source $V^a_{0\mu}(q)$, we obtain the vector current two-point function as

$$i\int d^4x\, e^{iqx}\langle J^a_\mu(x)J^b_\nu(0)\rangle = \delta_{ab}(q_\mu q_\nu - q^2 g_{\mu\nu})\,\Pi_V(-q^2)\,, \tag{3.16}$$

$$\Pi_V(-q^2) = -\frac{1}{g_5^2(-q^2)}\frac{\partial_z V(q,z)}{z}\bigg|_{z=\epsilon}\,, \tag{3.17}$$

Asymptotic form of $V(q,z)$ for large $-q^2$ is

$$V(q,z) = 1 + \frac{-q^2z^2}{4}\log(-q^2z^2) + \cdots\,, \tag{3.18}$$

which up to constant terms gives

$$\Pi_V(-q^2) = -\frac{1}{2g_5^2}\log(-q^2)\,. \tag{3.19}$$

On the other hand, the leading contribution of Π_V in QCD comes from the quark bubble,

$$\Pi_V(-q^2) = -\frac{N_c}{24\pi^2}\log(-q^2)\,, \tag{3.20}$$

where N_c denotes the number of colors. Comparing these two expressions, we obtain

$$g_5^2 = \frac{12\pi^2}{N_c}\,. \tag{3.21}$$

Now we see how the physical quantities are calculated in this model. We mode expand $V^a_\mu(x,z)$ by a complete set $\{\psi^{(n)}_\rho(z)\}$ as

$$V^a_\mu(x,z) = \sum_{n=1}^{\infty} V^{(n)a}_\mu(x)\,\psi^{(n)}_\rho(z)\,. \tag{3.22}$$

Here $\psi^{(n)}_\rho(z)$ satisfies the differential equation

$$\left[\partial_z\left(\frac{1}{z}\,\partial_z\right) + \frac{m^{(n)2}_\rho}{z}\right]\psi^{(n)}_\rho(z) = 0\,, \tag{3.23}$$

where $m^{(n)}_\rho$ is the eigenvalue, and $\psi^{(n)}_\rho$ satisfies the boundary conditions

$$\psi^{(n)}_\rho(\epsilon) = 0, \quad \partial_z\,\psi^{(n)}_\rho(z_m) = 0\,. \tag{3.24}$$

The eigenfunction $\psi_\rho^{(n)}$ satisfies the following orthonormal condition:

$$\int dz \frac{1}{z} \psi_\rho^{(n)}(z) \psi_\rho^{(m)}(z) = \delta_{nm} \,. \tag{3.25}$$

The lowest eigenvalue corresponds to the mass square of the ρ meson. The ρ decay constant defined by $\langle 0| \bar{q}\gamma_\mu t^a q |\rho^b\rangle = F_\rho \, \delta^{ab} \epsilon_\mu$ for the ρ meson with the polarization ϵ_μ is obtained as

$$F_\rho^2 = \frac{1}{g_5^2} \left[\frac{\psi_\rho'^{(1)}(\epsilon)}{\epsilon} \right]^2 \,, \tag{3.26}$$

which is the residue of the vector current two-point function.

Next, we consider the axial-vector sector. We introduce the axial-vector field A as

$$A = \frac{A_L - A_R}{2} \,. \tag{3.27}$$

The pion field $\pi^a(x,z)$ is defined as

$$X(x,z) = X_0(z) \, e^{i \, 2\pi^a(x,z) t^a} \,, \tag{3.28}$$

and we define $v(z)$ as

$$X_0(z) = \frac{1}{2} v(z) = \frac{1}{2}(m_q z + \sigma z^3) \,, \tag{3.29}$$

for later convenience. We work in the $A_z = 0$ gauge, and divide A_μ as

$$A_\mu = A_{\perp\mu} + \partial_\mu \varphi \,, \tag{3.30}$$

where the transverse part $A_{\perp\mu}$ satisfies $\partial^\mu A_{\perp\mu} = 0$. We mode expand $A^a_{\perp\mu}$ by a complete set $\{\psi_{a_1}^{(n)}(z)\}$ as

$$A^a_{\perp\mu}(x,z) = \sum_{n=1}^{\infty} A^{(n)a}_{\perp\mu}(x) \, \psi_{a_1}^{(n)}(z) \,. \tag{3.31}$$

Here $\psi_{a_1}^{(n)}(z)$ satisfies the differential equation

$$\left[\partial_z \left(\frac{1}{z} \partial_z \right) + \frac{m_{a_1}^{(n)2}}{z} - \frac{g_5^2 v^2(z)}{z^3} \right] \psi_{a_1}^{(n)}(z) = 0 \,, \tag{3.32}$$

where $m_{a_1}^{(n)}$ is the eigenvalue, and $\psi_{a_1}^{(n)}$ satisfies the boundary conditions

$$\psi_{a_1}^{(n)}(\epsilon) = 0, \quad \partial_z \psi_{a_1}^{(n)}(z_m) = 0\,, \tag{3.33}$$

The eigenfunction $\psi_{a_1}^{(n)}$ satisfies the following orthonormal condition

$$\int dz\, \frac{1}{z}\, \psi_{a_1}^{(n)}(z)\, \psi_{a_1}^{(m)}(z) = \delta_{nm}\,. \tag{3.34}$$

The lowest eigenvalue of the differential equation (3.32) with the boundary conditions (3.33) corresponds to the mass square of the a_1 meson. The a_1 decay constant is obtained as

$$F_{a_1}^2 = \frac{1}{g_5^2}\left[\frac{\psi_{a_1}'^{(1)}(\epsilon)}{\epsilon}\right]^2\,. \tag{3.35}$$

The pion decay constant defined by $\langle 0|\,\bar{q}\gamma_\mu\gamma_5 t^a q\,|\pi^b\rangle = i f_\pi\,\delta^{ab} q_\mu$ is obtained as

$$f_\pi^2 = -\frac{1}{g_5^2}\frac{\partial_z A(0,z)}{z}\bigg|_{z=\epsilon}\,, \tag{3.36}$$

which is the residue of the axial-vector current two-point function at the $m_\pi = 0$ limit. $A(0,z)$ is the solution of the differential equation

$$\left[\partial_z\left(\frac{1}{z}\,\partial_z\right) - \frac{g_5^2\, v^2(z)}{z^3}\right] A(0,z) = 0\,, \tag{3.37}$$

with the boundary conditions

$$A(0,\epsilon) = 1, \quad A'(0,z_m) = 0\,. \tag{3.38}$$

The pion mass m_π is obtained as the eigenvalue by solving the coupled differential equations

$$\partial_z\left(\frac{1}{z}\partial_z\right)\varphi^a + \frac{g_5^2\, v^2(z)}{z^3}(\pi^a - \varphi^a) = 0\,, \tag{3.39}$$

$$-m_\pi^2\,\partial_z\varphi^a + \frac{g_5^2\, v^2(z)}{z^2}\partial_z\pi^a = 0\,, \tag{3.40}$$

with the boundary conditions

$$\varphi(\epsilon) = 0\,, \quad \varphi'(z_m) = 0\,, \quad \pi(\epsilon) = 0\,. \tag{3.41}$$

Observable	Experiment (MeV)	Model (MeV)
m_{a_1}	1230 ± 40	1363
$\sqrt{F_\rho}$	348 ± 2	329
$\sqrt{F_{a1}}$	—	486
$g_{\rho\pi\pi}$	5.98 ± 0.01	4.48

Table 3.2: Results of the model for QCD observables. Experimental value are taken from Ref. [36].

The meson interactions are read from the nonbilinear terms in the 5d action. For example, the $\rho - \pi$ coupling is given by

$$g_{\rho\pi\pi} = g_5 \int dz\, \psi_\rho(z) \left(\frac{\varphi'^2(z)}{g_5^2 z} + \frac{v^2(z)(\pi(z) - \varphi(z))^2}{z^3} \right). \tag{3.42}$$

Now we show the quantitative predictions of this model. We use the experimental values of the ρ meson mass (775.8 MeV), the pion mass (139.6 MeV) and the pion decay constant (92.4 MeV) to fix the parameters as

$$z_m = 1/(323\text{MeV}), \tag{3.43}$$
$$m_q = 2.29\text{MeV}, \tag{3.44}$$
$$\sigma = (327\text{MeV})^3, \tag{3.45}$$

and take $N_c = 3$. The model predictions are summarized in Table 3.2. The results for m_{a_1} and $\sqrt{F_\rho}$ agree with the experimental values within 10%. However, this model underestimates $g_{\rho\pi\pi}$ by 30%. This may due to the fact that the 3-meson amplitude is sensitive to the F^3 term which is not included in the model.

3.2 The Sakai-Sugimoto model

The Sakai-Sugimoto model (SS model) [14] is a holographic model of 4d, large N_c QCD with massless quarks. It gives a holographic description of the spontaneous breaking of chiral symmetry $U(N_f)_L \times U(N_f)_R$ to the diagonal subgroup $U(N_f)_V$. The model predictions for the masses of the vector mesons and the pion charge radius are reasonably close to the experimental values. In this section, we briefly review the construction of the SS model and show its action.

The SS model is formulated by placing probe D8-branes into the D4-brane background. The D4-brane background consists of N_c D4-branes extended along $x^0, \cdots, x^4$ directions. The x^4 direction is compactified to S^1 with the anti-periodic boundary conditions for the fermions. The metric, dilaton ϕ and the RR three-form field C_3 in the D4-brane background are given as

$$ds^2 = \left(\frac{U}{R}\right)^{3/2}(\eta_{\mu\nu} + f(U)d\tau^2) + \left(\frac{R}{U}\right)^{3/2}\left(\frac{dU^2}{f(U)} + U^2 d\Omega_4^2\right),$$
$$e^{\phi} = g_s\left(\frac{U}{R}\right)^{3/4}, \quad F_4 = dC_3 = \frac{2\pi N_c}{V_4}\epsilon_4, \quad f(U) = 1 - \frac{U_{\rm KK}^3}{U^3}. \tag{3.46}$$

Here x^μ ($\mu = 0, 1, 2, 3$) and τ are the directions along which the D4-brane is extended, and U corresponds the radial direction transverse to the D4-brane. $\eta_{\mu\nu}$ is diag$(-, +, +, +)$. $d\Omega_4^2, \epsilon_4$ and $V_4 = 8\pi^2/3$ are the line element, the volume form and the volume of a unit S^4, respectively. R and $U_{\rm KK}$ are constant parameters. R is related to the string coupling g_s and string length l_s as $R^3 = \pi g_s N_c l_s^3$. From the definition of the function $f(U)$, U is bounded below as $U \geq U_{\rm KK}$. In order to avoid a conical singularity at $U = U_{\rm KK}$, τ must be a periodic variable with

$$\tau \sim \tau + 2\pi/M_{\rm KK}, \quad M_{\rm KK} = \frac{3}{2}\frac{U_{\rm KK}^{1/2}}{R^{3/2}}, \tag{3.47}$$

where $M_{\rm KK}$ is the cutoff scale of the theory. This D4-brane background yields a holographic dual of 4d pure Yang-Mills theory at low energies, $E \ll M_{\rm KK}$ [37]. The Yang-Mills coupling $g_{\rm YM}$ at $M_{\rm KK}$ can be read off of the DBI action of the D4-brane compactified on the S_1 as $g_{\rm YM}^2 = 2\pi M_{\rm KK} g_s l_s$. The parameters $R, U_{\rm KK}$ and g_s are expressed in terms of $M_{\rm KK}, l_s$ and the 't Hooft couplong $\lambda = g_{\rm YM}^2 N_c$ as

$$R^3 = \frac{1}{2}\frac{\lambda l_s^2}{M_{\rm KK}}, \quad U_{\rm KK} = \frac{2}{9}\lambda M_{\rm KK} l_s^2, \quad g_s = \frac{1}{2\pi}\frac{\lambda}{N_c M_{\rm KK} l_s}. \tag{3.48}$$

This supergravity description is valid for $\lambda \gg 1$.

In order to add N_f flavors of quarks to the supergravity dual of the Yang-Mills theory described by the background (3.46), we place N_f probe D8-branes extended along $x^\mu (\mu = 0, 1, 2, 3)$, the S^4 directions, and one of the directions in the (U, τ) plane. Here we adopt the probe approximation, assuming $N_c \gg N_f$, and ignore the backreaction from the D8-branes to the D4-brane background. The induced metric on the D8-brane embedded in the D4-background (3.46) with $U = U(\tau)$ is given by

$$ds_{\rm D8}^2 = \left(\frac{U}{R}\right)^{3/2}\eta_{\mu\nu}dx^\mu dx^\nu + \left[\left(\frac{U}{R}\right)^{3/2} f(U) + \left(\frac{R}{U}\right)^{3/2}\frac{U'^2}{f(U)}\right]d\tau^2 + U^2 d\Omega_4^2, \tag{3.49}$$

where $U' = (d/d\tau)U$. To describe the D8-brane, it is convenient to introduce new coordinate (y, z) defined by

$$(y, z) = (r\cos(M_{\rm KK}\tau), r\sin(M_{\rm KK}\tau)) \ , \tag{3.50}$$

where

$$U^3 = U_{\rm KK}^3 + U_{\rm KK} r^2 \ . \tag{3.51}$$

We consider the D8-brane placed at $y = 0$ and extended along the z direction. Thus,

$$U^3 = U_{\rm KK}^3 + U_{\rm KK} z^2 \equiv U_z^3(z) \, , \tag{3.52}$$

and (3.50) is written as

$$ds_{D8}^2 = \left(\frac{U_z}{R}\right)^{3/2} \eta_{\mu\nu}\, dx^\mu dx^\nu + \left(\frac{R}{U_z}\right)^{3/2} \left(\frac{dU_z^2}{f(U_z)} + U_z^2 d\Omega_4^2\right) . \tag{3.53}$$

Next, we consider the gauge field on the probe D8-brane. The gauge field on the D8-brane has nine components, $A_\mu (\mu = 0, 1, 2, 3)$, A_z and A_α ($\alpha = 5, 6, 7, 8$ are the coordinates on the S^4). Since QCD does not have the $SO(5)$ symmetry corresponding to the rotation of S^4, we concentrate on the $SO(5)$ singlet states. Therefore, we here set $A_\alpha = 0$ and assume that A_μ and A_z are independent of the coordinate on the S^4. The effective action on the D8-brane consists of two parts — the DBI action and the Chern-Simons term. Let us first consider the DBI action for the $U(1)_V$ gauge field, which is the subgroup of the $U(N_f)_V$ group. The DBI action is given by

$$S_{\rm DBI} = -T \int d^9x\, e^{-\phi} \sqrt{-\det(g_{MN} + 2\pi\alpha' F_{MN})} \, , \tag{3.54}$$

where

$$T = \frac{2\pi}{(2\pi l_s)^9} \, , \quad \alpha' = l_s^2 \, . \tag{3.55}$$

This action reduces to the 5d action as

$$S_{\rm DBI} = -\tilde{T}(2\pi\alpha')^2 \int d^4x\, dz \left[\frac{R^3}{4U_z} F_{\mu\nu}^2 + \frac{9}{8}\frac{U_z^3}{U_{\rm KK}} F_{\mu z}^2\right] + O(F^4) \, , \tag{3.56}$$

where

$$\tilde{T} = \frac{2}{3} R^{3/2} U_{\rm KK}^{1/2} T V_4 \frac{1}{g_s} \, . \tag{3.57}$$

Let us then consider the DBI action for the $U(N_f)_V$ gauge field. The leading terms of the DBI action in this case are given by the non-Abelian generalization of (3.56) as

$$S_{\rm DBI} = -\tilde{T}(2\pi\alpha')^2 \int d^4x\, dz\ {\rm tr}\left[\frac{R^3}{4U_z}F_{\mu\nu}^2 + \frac{9}{8}\frac{U_z^3}{U_{\rm KK}}F_{\mu z}^2\right], \tag{3.58}$$

where $F_{MN} = \partial_M A_N - \partial_N A_M - [A_M, A_N]$ is the field strength of the $U(N_f)$ gauge field A_M ($M = 0, 1, 2, 3, z$) on the D8-brane. Note that (3.58) is often expressed as

$$S_{\rm DBI} = -\kappa \int d^4x\, dz\ {\rm tr}\left[\frac{1}{2}K^{-1/3}F_{\mu\nu}^2 + KF_{\mu z}^2\right], \tag{3.59}$$

with

$$\kappa = \frac{\lambda N_c}{216\pi^3}, \quad K(z) = 1 + z^2, \tag{3.60}$$

by using the fact that we can set

$$M_{\rm KK} = 1, \quad l_s^2 = \frac{9}{2\lambda}, \tag{3.61}$$

without loss of generality. The Chern-Simons term is written as

$$S_{\rm CS} = \frac{i\,N_c}{24\pi^2}\int \omega_5(A), \tag{3.62}$$

where $\omega_5(A)$ is the Chern-Simons five-form written in terms of the five-dimensional differential form $A = A_\mu\, dx^\mu + A_z\, dz$ as

$$\omega_5(A) = {\rm tr}\left(AF^2 - \frac{1}{2}A^3F + \frac{1}{10}A^5\right). \tag{3.63}$$

The 5d Yang-Mills+Chern-Simons action $S = S_{\rm DBI} + S_{\rm CS}$ is the action of the SS model, and it is the low energy effective theory for mesons.

3.3 Baryons in holographic QCD

The success of the SS model in describing the meson phenomenology provides us with a strong motivation to extend it to the baryon sector. The pioneering works are presented by Nawa *et al.* [38], Hong *et al.* (HRYY model) [39] and by Hata *et al.* [40]. In Ref. [40], they find an instanton solution of the static limit of the 5d Yang-Mills theory which carries a unit baryon number, and quantize it to obtain

the baryon mass spectra. This approach is applied to study the static properties of baryons [41] and the nuclear force [42]. In this section, we review the HRYY model, which is more tractable in treating many-body physics. In Chapter 5, we will use this model to study baryon many-body systems.

In the context of the AdS/CFT correspondence, a baryon is realized as a baryon vertex [43, 44], which consists of a D-brane wrapped on a compact subspace and the N_c fundamental strings connecting the flavor brane and the D-brane. In the SS model, a D4-brane wrapped on S^4 corresponds to a baryon vertex, which is realized as an instanton in the gauge theory on the D8-brane. There are N_c fundamental strings connecting the D4-brane with the D8-brane. Since each end point of the fundamental strings carries a unit charge (quark charge) with respect to the $U(1)$ gauge field on the D8-brane, a D4-brane wrapped on S^4 looks like an object with charge N_c.

Using the fact that the size of the instanton is very small in the large 't Hooft coupling limit, we treat it as a point-like field in 5d space. We introduce a 5d Dirac spinor B for the spin $1/2$ baryon. We write down an action in 5d space, whose metric is give by

$$ds_{5d}^2 = H(w)\,(dw^2 + \eta_{\mu\nu}dx^\mu dx^\nu)\,, \tag{3.64}$$

where $\eta_{\mu\nu}$ is diag$(-,+,+,+)$. The non-compact 5d part of the induced metric on the D8-brane (3.53) is transformed to the conformally flat metric (3.64) by the coordinate transformation

$$w = \pm \int_{U_{\rm KK}}^{U} dU' \, \frac{R^{3/2}}{\sqrt{U'^3 - U_{\rm KK}^3}}\,, \tag{3.65}$$

with

$$H(w) = \left(\frac{U(w)}{R}\right)^{3/2}\,. \tag{3.66}$$

Note that the boundaries are located at $w = \pm w_{\rm max}$, where

$$\begin{aligned} w_{\rm max} &= \int_{U_{\rm KK}}^{\infty} dU \, \frac{R^{3/2}}{\sqrt{U^3 - U_{\rm KK}^3}} \\ &= \frac{1}{M_{\rm KK}}\frac{3}{2}\int_1^\infty d\tilde{U}\,\frac{1}{\sqrt{\tilde{U}^3-1}} \qquad \left(\tilde{U} = \frac{U}{U_{\rm KK}}\right) \\ &\simeq \frac{3.64}{M_{\rm KK}} < \infty\,. \end{aligned} \tag{3.67}$$

The action for the baryon is written as

$$S_B = \int d^4x \int dw\ \sqrt{-g}\left(i\,\bar{B}\,e_A^M\Gamma^A D_M B - m_b(w)\bar{B}B\right). \tag{3.68}$$

where $m_b(w)$ is the 5d mass of the baryon. The w dependence of $m_b(w)$ reflects the curvature of the original geometry. g_{MN} $(M,N = 0,1,2,3,5)$ is the metric of (3.64), and the vielbein e_M^A is

$$e_M^A = \sqrt{H(w)}\,\delta_M^A\,, \tag{3.69}$$

which satisfies

$$g_{\rm MN} = e_M^A e_N^B\,\eta_{AB}\,, \tag{3.70}$$

where $\eta_{AB} = \mathrm{diag}(-,+,+,+,+)$. Γ^M are written in terms of the 4d Dirac matrices as $\Gamma^\mu = \gamma^\mu$ $(\mu = 0,1,2,3)$ and $i\Gamma^w = \gamma^5$. The covariant derivative is given by

$$\begin{aligned} D_M &= \partial_M + \frac{i}{4}\,\omega_M^{AB}\,\Gamma_{AB} - i\,A_M\,, \\ \Gamma^{AB} &= \frac{1}{2i}\,[\Gamma^A,\Gamma^B]\,, \end{aligned} \tag{3.71}$$

where ω_M^{AB} denote the spin connection. The non-vanishing components of the spin connection are

$$\omega_M^{5A} = -\omega_M^{A5} = -\frac{H'(w)}{2H(w)}\,\delta_M^A\,. \tag{3.72}$$

By redefining the baryon field and its 5d mass as

$$H(w)\,B \to B\,, \tag{3.73}$$

$$\sqrt{H(w)}\,m_5(w) \to m_5(w)\,, \tag{3.74}$$

the action (3.68) reduces to the form

$$S_B = \int d^4x \int dw\,\left[i\,\bar{B}\Gamma^M(\partial_M - i\,A_M)B - m_5(w)\,\bar{B}B\right]. \tag{3.75}$$

The 5d mass $m_b(w)$ should be identified as the energy of a D4-brane wrapped on S^4 localized at the position w. From the DBI action of the D4-brane, this energy is found to be

$$m_B^{(0)}\left(\frac{U(w)}{U_{\rm KK}}\right), \tag{3.76}$$

where $m_B^{(0)}$ is the energy of a D4-brane wrapped on S^4 located at $w = 0$

$$m_B^{(0)} = \frac{\lambda N_c}{27\pi} M_{\rm KK} \,. \tag{3.77}$$

In addition, there is a correction to the instanton mass from the Coulomb repulsion among the charges of the N_c fundamental strings as

$$m_0^e = \frac{1}{3} m_B^{(0)} (M_{\rm KK}\, \rho_{\rm baryon})^2 = \frac{\sqrt{2 \cdot 3^7 \cdot \frac{\pi^2}{5}}}{3\lambda}\, m_B^{(0)} \,, \tag{3.78}$$

where $\rho_{\rm baryon}$ denotes the size of the instanton

$$\rho_{\rm baryon}^2 = \frac{\sqrt{2 \cdot 3^7 \cdot \frac{\pi^2}{5}}}{M_{\rm KK}^2\, \lambda} \,. \tag{3.79}$$

This Coulomb repulsion prevents an instanton from shrinking to zero-size. We use

$$\begin{aligned} m_b(w) &= m_B^{(0)} \left(\frac{U(w)}{U_{\rm KK}} \right) + \frac{\sqrt{2 \cdot 3^7 \cdot \frac{\pi^2}{5}}}{3\lambda}\, m_B^{(0)} \\ &= M_{\rm KK} \left[\frac{\lambda\, N_c}{27\pi} \left(\frac{U(w)}{U_{\rm KK}} \right) + \sqrt{\frac{2}{15}}\, N_c \right] , \end{aligned} \tag{3.80}$$

in the following calculations.

Next, we see how the baryon mass of this model is obtained. We mode expand the 5d Dirac field $B(x, w)$ by $f_{R,L}(w)$ as

$$B(x, w) = f_R(w)\, \psi_R(x) + f_L(w)\, \psi_L(x) \,. \tag{3.81}$$

We can always take $f_{R,L}(w)$ to be real functions by being absorbed the phase factors by $\psi_{R,L}(w)$. $f_{R,L}(w)$ satisfy the differential equations

$$-\partial_w f_R + m_b(w) f_R = m_B f_L \,, \tag{3.82}$$

$$\partial_w f_L + m_b(w) f_L = m_B f_R \,, \tag{3.83}$$

where m_B is the eigenvalue of the equations. In holographic models, the infinite tower of baryons are interpreted as Kaluza-Klein states associated with the fifth

direction. $B(x,w)$ is expanded by the complete set $\{f_{R,L}^{(n)}\}$, where each $f_{R,L}^{(n)}$ corresponds to the baryon in nth excited state. In this section, however, we neglect the heavier modes, or the baryons in the excited states. We thus leave $f_{R,L}(w)$ and focus on the baryon in the ground state. Note that $\psi_{R,L}$ in (3.81) are the components of 4d Dirac spinor ψ, which are defined as

$$\psi_R = \frac{1+\gamma^5}{2}\psi\,, \quad \psi_L = \frac{1-\gamma^5}{2}\psi\,. \tag{3.84}$$

Substituting the expansion (3.81) into the 5d baryon action (3.75), the kinetic term and the mass term are written as

$$\begin{aligned} i\bar{B}\Gamma^M\partial_M B = &-f_R\partial_w f_L\,(\bar{\psi}_R\psi_L) + f_L\partial_w f_R\,(\bar{\psi}_L\psi_R) \\ &+ f_R^2\,(\bar{\psi}_R i\gamma^\mu\partial_\mu\psi_R) + f_L^2\,(\bar{\psi}_L i\gamma^\mu\partial_\mu\psi_L)\,, \end{aligned} \tag{3.85}$$

and

$$m_b(w)\,\bar{B}B = m_b(w)\,f_R f_L\,(\bar{\psi}_R\psi_L + \bar{\psi}_L\psi_R)\,, \tag{3.86}$$

respectively. The parity transformation for $\psi(x,w)$ is

$$\psi(\mathbf{x},t) \to \gamma^0\psi(-\mathbf{x},t)\,, \tag{3.87}$$

or

$$\psi_{R,L}(\mathbf{x},t) \to \gamma^0\psi_{L,R}(-\mathbf{x},t)\,, \tag{3.88}$$

thus, the 5d action is invariant under the parity transformation when

$$\begin{aligned} &\int dw\; f_R(w)\,\partial_w f_L(w) = \int dw\; f_L(w)\,(-\partial_w) f_R(w) = \int dw\; f_L(-w)\,\partial_w f_R(-w)\,, \\ &\int dw\; f_R(w)\; f_R(w) = \int dw\; f_L(w)\; f_L(w) = \int dw\; f_L(-w)\; f_L(-w)\,, \end{aligned} \tag{3.89}$$

are satisfied. All of these conditions are realized when we choose

$$f_R(w) = \pm f_L(-w)\,. \tag{3.90}$$

By using the differential equations (3.82) and (3.83), we can rewrite the kinetic term plus the mass term as

$$i\bar{B}\Gamma^M\partial_M B - m_b(w)\,\bar{B}B = f_R^2\,\bar{\psi}_R(i\gamma^\mu\partial_\mu - m_B)\psi_R + f_L^2\,\bar{\psi}_L(i\gamma^\mu\partial_\mu - m_B)\psi_L\,. \tag{3.91}$$

Integrating over w direction with the normalization condition

$$\int dw\, f_R^2(w) = \int dw\, f_L^2(w) = 1\,, \tag{3.92}$$

we obtain the 4d baryon action

$$\int d^4x\, \bar{\psi}(i\gamma^\mu \partial_\mu - m_B)\psi\,. \tag{3.93}$$

Therefore, we can interpret m_B as the mass of a baryon.

When we define

$$f = f_L + f_R\,, \tag{3.94}$$
$$\tilde{f} = f_L - f_R\,, \tag{3.95}$$

the differential equations (3.82) and (3.83) are written as

$$\partial_w f - (m_b(w) + m_B)\ \tilde{f} = 0\,, \tag{3.96}$$
$$\partial_w \tilde{f} - (m_b(w) - m_B)\ f = 0\,, \tag{3.97}$$

and the condition (3.90) becomes

$$f(w) = \pm f(-w)\,. \tag{3.98}$$

The boundary conditions for the $f(w) = f(-w)$ case are

$$f'(0) = 0\,(\text{regular at}\, w = 0)\,, \quad f(\pm w_{\text{max}}) = 0\,(\text{normalizable})\,, \tag{3.99}$$

and those for the $f(w) = -f(-w)$ case are

$$f(0) = 0\,(\text{regular at}\, w = 0)\,, \quad f(\pm w_{\text{max}}) = 0\,(\text{normalizable})\,. \tag{3.100}$$

The baryon mass m_B is obtained as the eigenvalue of the eigenvalue equations (3.96) and (3.97). In order to obtain the mass of the baryon in the ground state, we find the lowest positive eigenvalue with the boundary condition (3.99), which is the same value (up to sign) as the lowest negative eigenvalue with (3.100).

The results for the baryon mass m_B for various values of λN_c are listed in Table 3.3. This shows that the baryon mass increases as the 't Hooft coupling λ becomes larger. This is due to the fact that the 5d mass of the baryon $m_b(w)$ is proportional to λ. If we fix two parameters of the model in the same way as in

λN_c	$m_B/M_{\rm KK}$
10	1.37
20	1.52
30	1.66
40	1.80
50	1.93
60	2.06
80	2.32

Table 3.3: Numerical results for the baryon mass.

Ref. [14]. We fit the values of $M_{\rm KK}$ and λN_c to fit the experimental values of the ρ meson mass and the pion decay constant as

$$M_{\rm KK} = 949\,{\rm MeV}, \quad \lambda N_c = 50\,. \tag{3.101}$$

Then, the baryon mass is estimated as

$$m_B = 1.93 M_{\rm KK} = 1.83{\rm GeV}\,, \tag{3.102}$$

which is about twice as heavy as the experimental values of the nucleon mass. This suggests that it is difficult to reproduce meson and baryon mass spectra simultaneously in this model. Such a situation is also seen in other holographic models with the instanton baryons [40] and in the Skyrme model [45].

Chapter 4

$\rho - a_1$ mixing in dense baryonic matter

In this chapter, we report our study [1] on the $\rho - a_1$ mixing in dense baryonic matter. We use a holographic model in the bottom-up approach to investigate the mixing.

4.1 The $\rho - a_1$ mixing

At finite baryon number density, charge conjugation invariance is violated because the number of baryons is larger than that of anti-baryons. There, the vector (ρ) and the axial-vector (a_1) mesons with finite momenta mix though a mixing term [46, 47]

$$\mathcal{L}_{\rm mix} = C\,\epsilon^{0\nu\lambda\sigma}\left[\partial_\nu V_\lambda \cdot A_\sigma + \partial_\nu A_\lambda \cdot V_\sigma\right] , \tag{4.1}$$

which violates charge conjugation invariance, but preserves parity invariance. The coefficient C determines the strength of the mixing. This means that the dispersion relation of these mesons are modified at finite density.

In this study, we use a holographic model in the bottom-up approach to observe the density dependence of the dispersion relations of these modes. An example of this study in holographic QCD is shown in Ref. [46]. They construct an effective action in AdS_5 space, whose metric is given by

$$ds^2 = \frac{1}{z^2}\left(-dz^2 + dx^\mu dx_\mu\right), \quad (\epsilon \le z \le z_m), \tag{4.2}$$

[1] This study has been done in collaboration with Masayasu Harada (Nagoya University, Japan) with the discussions with Youngman Kim (APCTP, Korea).

and add the Chern-Simons term which causes the $\rho - a_1$ mixing at finite density. In Ref. [46], they succeeded in estimating the strength of the mixing C. In the present analysis, we study how the following two contributions affect the mixing. One is the backreaction of the matter to spacetime geometry. The 5d space is distorted by dense matter, so the true metric deviates from (4.2) as the density grows. This means that the analysis using the metric (4.2) is reliable only at the low density region. Another is the contributions from the mixing to the higher excited states. The ρ meson can mix not only with the a_1 meson, but also with its excited states $a_1', a_1'', \cdots$. The aim of this study is to observe how these ingredients affect the $\rho - a_1$ mixing.

4.2 The model

We construct a model based on the hard-wall model, which we reviewed in Section 3.1. We set a UV boundary at $z = \epsilon$, and an IR cutoff at $z = z_m$ in the fifth direction. To construct a 5d dual of dense QCD, we introduce a 5d $U(1)$ gauge field $A_M(x, z)$ which corresponds to the quark number current in QCD. In this study, we express density in terms of the quark number density n_q and the quark chemical potential μ_q, which are related to the baryon number density n_B and the baryon chemical potential μ_B as

$$n_q = N_c\, n_B\,, \tag{4.3}$$

$$\mu_q = \frac{1}{N_c}\,\mu_B\,, \tag{4.4}$$

where N_c denotes the number of colors.

We work in the $A_z(x, z) = 0$ gauge, and replace the gauge field with the mean field as

$$A_0(x, z) \to A_0(z)\,, \quad A_i(x, z) \to 0\,. \tag{4.5}$$

We impose

$$A_0(\epsilon) = \mu\,, \tag{4.6}$$

where μ is the quark chemical potential.

It is shown in Ref. [48] that the metric

$$ds^2 = \frac{1}{z^2}\left(-\frac{1}{f(z)}\,dz^2 + f(z)\,dt^2 - dx_i^2\right), \quad f(z) = 1 + q^2\, z^6\,, \tag{4.7}$$

and the mean field

$$A_0(z) = \mu_q - Q z^2 \,, \tag{4.8}$$

with

$$q^2 = \frac{2\kappa^2}{3g^2} Q^2 \,, \tag{4.9}$$

satisfy the Einstein equation

$$R_{MN} - \frac{1}{2} G_{MN} R - G_{MN} \left(-\frac{1}{6}\right) = -\frac{\kappa^2}{g_5^2} \left(F_{MP} F_N^P - \frac{1}{4} G_{MN} F_{PQ} F^{PQ} \right) , \tag{4.10}$$

and the Maxwell equation

$$\partial_M \sqrt{G}\, G^{MP} G^{NQ} F_{PQ} = 0 \,, \tag{4.11}$$

simultaneously. Thus, the backreaction of the matter to gravity is correctly introduced in (4.7). Note that the metric (4.7) reduces to the simple AdS_5 metric (4.2) for $f(z) = 1$. In the following calculations, we use the metric (4.7) and then compare the results with the $f(z) = 1$ case.

We use a 5d action

$$S_5 = \int d^4x\, dz\, \sqrt{G}\, \mathrm{Tr} \left[|\, D X \,|^2 + 3 \,|\, X \,|^2 - \frac{1}{4g_5^2} (F_L^2 + F_R^2) \right] , \tag{4.12}$$

and add a Chern-Simons term

$$S_{\mathrm{CS}} = \frac{i N_c}{24\pi^2} \int \left(\omega_5 (A_L) - \omega_5 (A_R) \right) , \tag{4.13}$$

which contains a $\rho - a_1$ mixing term

$$\frac{N_c}{8\pi^2} Q \int d^4x\, dz\, z\, \epsilon^{ijk} \left(V_i^a\, \partial_j A_k^a + A_i^a\, \partial_j V_k^a \right) . \tag{4.14}$$

$F_{L,R}$ in (4.12) is the field strength tensor of the $U(2)_{L,R}$ gauge field $A_{L,R}$ which consists of the $U(1)_{L,R}$ part $\hat{A}_{L,R}$ and the $SU(2)_{L,R}$ part $A_{L,R}^a$ as

$$A_{L,R} = \hat{A}_{L,R}\, \hat{t} + A_{L,R}^a\, t^a \,, \tag{4.15}$$

where $\hat{t}$ and t^a are the generators of $U(1)$ and $SU(2)$, respectively. Therefore, (4.12) is $U(2)_L \times U(2)_R$ gauge invariant. In (4.14), we defined the vector and the axial-vector fields as

$$V = \frac{1}{2} (A_L + A_R) \,, \quad A = \frac{1}{2} (A_L - A_R) \,. \tag{4.16}$$

Q is proportional to the quark number density n_q as

$$n_q = \frac{Q}{g_5^2}\,, \tag{4.17}$$

which is found by differentiating the on-shell action with respect to the quark chemical potential μ_q [46]. Therefore, the transverse modes of the ρ and the a_1 mesons with finite momenta mix through (4.14) at finite density.

In the following analysis, we take the degenerated mass for up and down quarks $m_u = m_d = m_q$. We define $v(z)$ as

$$X(z) = \frac{1}{2}\, v(z) \begin{bmatrix} 1 & 0 \\ 0 & 1 \end{bmatrix}. \tag{4.18}$$

Then, the equation of motion for $v(z)$ is defined as

$$\left[\partial_z^2 + \frac{z\, f'(z) - 3\, f(z)}{z\, f(z)}\, \partial_z + \frac{3}{z^2\, f(z)}\right] v(z) = 0\,. \tag{4.19}$$

The solution is given by

$$v(z) = m_q\, z\ {}_2F_1\left(\frac{1}{6}, \frac{1}{2}, \frac{2}{3}, -q^2 z^6\right) + \sigma\, z^3\, {}_2F_1\left(\frac{1}{2}, \frac{5}{6}, \frac{4}{3}, -q^2 z^6\right). \tag{4.20}$$

4.3 The dispersion relation of the $\rho - a_1$ mixture

We work in the $V_z = A_z = 0$ gauge, and choose the momentum to the third direction as

$$k = (\omega, 0, 0, k_3)\,. \tag{4.21}$$

We mode expand the transverse modes of the vector ($V_{1,2}$) and the axial-vector ($A_{2,1}$) fields by the complete sets $\{\psi_\rho^{(n)}(z)\}$ and $\{\psi_{a_1}^{(n)}(z)\}$ as

$$V_1^a(k,z) = V_2^a(k,z) = \sum_{n=1}^{\infty} V_T^{(n)\,a}(k)\, \psi_\rho^{(n)}(z)\,, \tag{4.22}$$

$$i\, A_2^a(k,z) = -i\, A_1^a(k,z) = \sum_{n=1}^{\infty} V_T^{(n)\,a}(k)\, \psi_{a_1}^{(n)}(z)\,. \tag{4.23}$$

$\psi_\rho^{(n)}(z)$ and $\psi_{a_1}^{(n)}(z)$ satisfy the differential equations

$$\partial_z\left(\frac{1}{z}\,f(z)\,\partial_z\right)\psi_\rho^{(n)}(z) = -\frac{1}{z}\left(\frac{\omega^{(n)\,2}}{f(z)} - k_3^2\right)\psi_\rho^{(n)}(z) - \left(\frac{N_c}{4\pi^2}\,g_5^2\,Q\right) z\,k_3\,\psi_{a_1}^{(n)}(z)\,, \tag{4.24}$$

$$\left[\partial_z\left(\frac{1}{z}\,f(z)\,\partial_z\right) - g_5^2\,\frac{v^2(z)}{z^3}\right]\psi_{a_1}^{(n)}(z) = -\frac{1}{z}\left(\frac{\omega^{(n)\,2}}{f(z)} - k_3^2\right)\psi_{a_1}^{(n)}(z) - \left(\frac{N_c}{4\pi^2}\,g_5^2\,Q\right) z\,k_3\,\psi_\rho^{(n)}(z)\,, \tag{4.25}$$

where $\omega^{(n)}$ is the eigenvalue. The eigenfunctions $\psi_\rho^{(n)}(z)$ and $\psi_{a_1}^{(n)}(z)$ satisfy the orthonormal condition

$$\int dz\,\frac{1}{z\,f(z)}\left[\psi_\rho^{(n)}(z)\,\psi_\rho^{(m)}(z) - \psi_{a_1}^{(n)}(z)\,\psi_{a_1}^{(m)}(z)\right] = \delta_{nm}\,. \tag{4.26}$$

Substituting the expansions (4.22) – (4.23) into the action $S_5 + S_{\rm CS}$, the transverse part becomes

$$(S_5 + S_{\rm CS})_{\rm transverse} = 2\sum_{n=1}^{\infty}\int\frac{d^4k}{(2\pi)^4}\,\frac{1}{2}\,\frac{1}{g_5^2}\,(\omega^2 - \omega^{(n)\,2})\,V_T^{(n)\,a}(k)\,V_T^{(n)\,a}(-k)\,. \tag{4.27}$$

Thus, we can interpret the eigenvalue $\omega^{(n)}$ of the differential equations (4.24) – (4.25) as the energy of the $\rho - a_1$ mixture in the $(n-1)$ th excited state. In this study, we observe the dispersion relation of the $\rho - a_1$ mixture in the ground state by finding the eigenvalue $\omega^{(1)}\,(k_3)$ of the differential equations (4.24) – (4.25) with the boundary conditions

$$\psi_{\rho,a_1}^{(1)}(\epsilon) = 0, \quad \partial_z\,\psi_{\rho,a_1}^{(1)}(z_m) = 0\,, \tag{4.28}$$

for each momentum k_3.

Now we show the numerical results. We use the same parameter set as in Section 3.1, i.e.

$$g_5^2 = \frac{12\,\pi^2}{N_c}\,, \tag{4.29}$$

$$z_m = 1/(323\text{MeV})\,, \tag{4.30}$$

$$m_q = 2.29\text{MeV}\,, \tag{4.31}$$

$$\sigma = (327\text{MeV})^3\,, \tag{4.32}$$

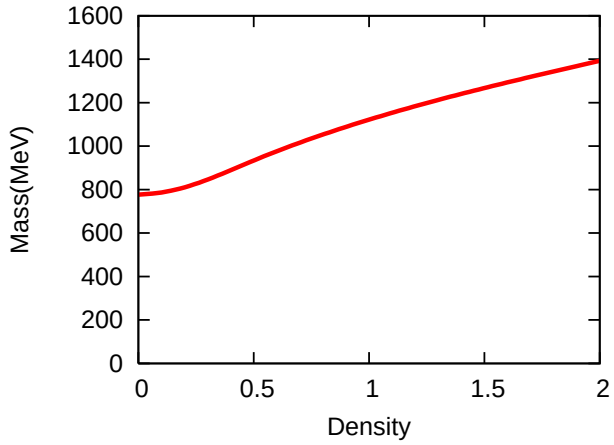

Figure 4.1: Density dependence of the ρ meson mass. The horizontal axis represents the baryon number density normalized by the normal nuclear matter density, n_q/n_0.

and fix the Newton constant by matching the free energy of QCD with that of the gravity theory [48] as

$$\frac{1}{\kappa^2} = \frac{2\,N_c^2}{45\pi^2}\,, \tag{4.33}$$

and take $N_c = 3$. We use the quark number density of the normal nuclear matter

$$n_0 = 3.69 \times 10^6\,\mathrm{MeV}^3\,, \tag{4.34}$$

to normalize the quark number density n_q.

Figure 4.1 shows the density dependence of the ρ meson mass, which is already studied in Ref. [48]. The ρ meson mass increases as the density grows. If we take $f(z) = 1$, the ρ meson mass does not change with the density, which means that the mass increase in Figure 4.1 is caused by the backreaction.

Figure 4.2 shows the dispersion relation of the $\rho - a_1$ mixture for $n_q/n_0 = 0.1, 0.5$ and 1.0. For $n_q/n_0 = 0.1$, the dispersion relation is consistent with the Klein-Gordon type dispersion relation (KG), $\omega(k_3) = \sqrt{m^2 + k_3^2}$. For $n_q/n_0 = 0.5$, however, the dispersion relation deviates from KG, and the energy is shifted downward due to the $\rho - a_1$ mixing [47]. The energy is more shifted downward as the density grows, and for $n_q/n_0 = 1.0$, it drops to 0 at $k_3 = 540$ MeV — the condensation of the ρ and a_1 mesons occurs. This condensation breaks rotational invariance in 3d space.

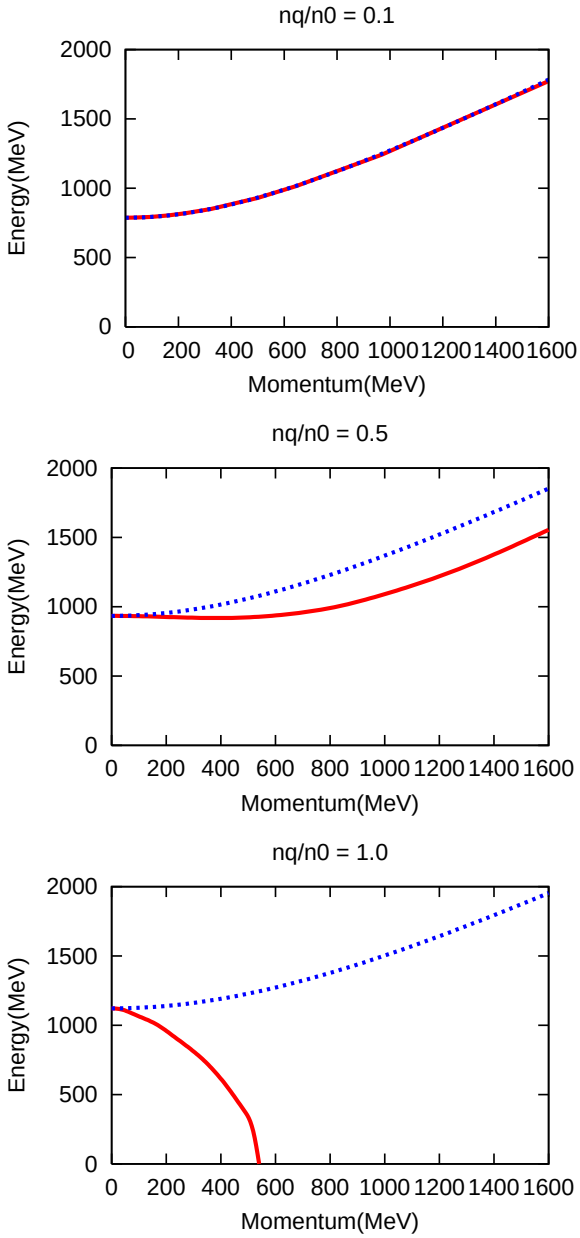

Figure 4.2: The dispersion relation of the $\rho - a_1$ mixture for $n_q/n_0 = 0.1, 0.5, 1.0$. The solid line indicates the dispersion relation of the $\rho - a_1$ mixture, and the dashed line indicates the Klein-Gordon type dispersion relation, $\omega(k_3) = \sqrt{m^2 + k_3^2}$.

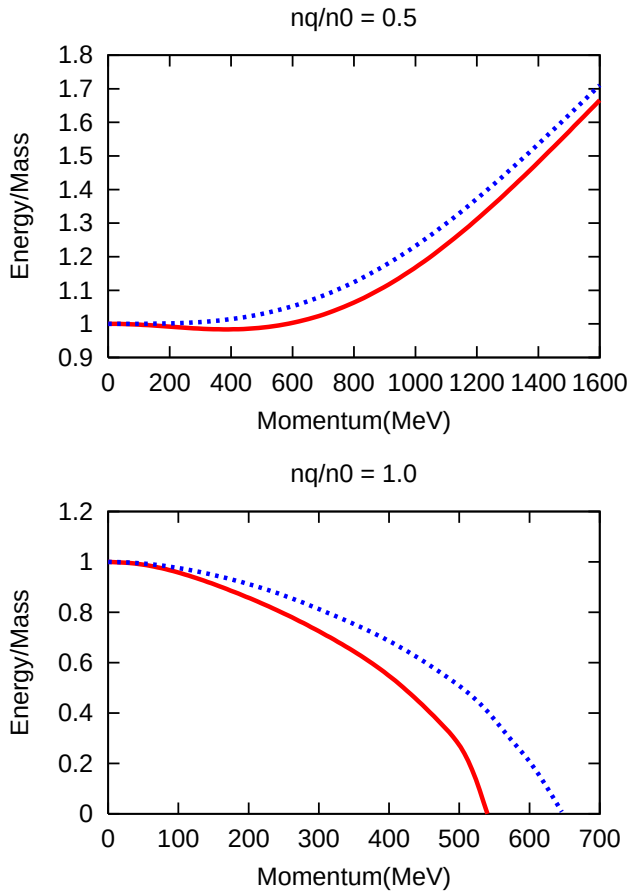

Figure 4.3: The dispersion relations of the $\rho - a_1$ mixture with (solid) and without (dashed) backreaction. The vertical axis represents the energy of the $\rho - a_1$ mixture normalized by the ρ meson mass.

Figure 4.3 shows the effect of the backreaction on the dispersion relation. It is shown that the energy is shifted downward due to the backreaction more than the case without backreaction. Thus, we find that the mixing becomes even stronger when we take the backreaction into account.

4.4 Discussions

We have discussed the $\rho - a_1$ mixing in dense baryonic matter by using a holographic model in the bottom-up approach. We have used the metric proposed in Ref. [48] in which the backreaction of the matter to gravity is taken into account. The energy of the $\rho - a_1$ mixture in the ground state is shifted downward due to the mixing, which becomes stronger as the density grows. We have also seen that the mixing becomes even stronger when we take the backreaction into account.

Surprisingly, it is suggested that the vector meson condensation occurs at the normal nuclear matter density. This possibility is also mentioned in Ref. [46]. The situation can change depending on how we fix the parameters [49], or we include higher order terms into the model action. It is of particular interest to explore how the situation changes when we include dynamical baryons into the model. The existence of dynamical baryons does affect the mean field $A_0(z)$ and thus contributes the mixing term. It is important to obtain a holographic model at finite density including dynamical baryons, and we will address this issue in the next chapter.

Chapter 5

Holographic mean-field theory for baryon many-body systems

In this chapter, we report our study in Ref. [50].

The current framework of the AdS/CFT correspondence still has room for improvement in dealing with the systems at finite baryon density. It can be summarized as follows: 1) dynamical baryons at finite density have not been satisfactorily incorporated, and 2) the application of the GKP-Witten prescription [12, 13] to relate the baryon chemical potential to the baryon density has an ambiguity in the grand canonical ensemble.

In this chapter, we shall propose a new approach, a holographic mean-field theory for fermions, to resolve these two problems. The self-consistent incorporation of dynamical baryons in our mean-field approach provides an eigenvalue equation which eliminates the ambiguity. We apply our approach to the HRYY model in Section 3.3 and present the relation between the chemical potential and the baryon density.

5.1 Baryonic matter in holographic QCD

The quarks are realized as fundamental strings attached to the flavor brane in the gravity dual [51]. Each end point of the strings carries a unit charge with respect to a $U(1)$ gauge field on the flavor brane, and the quark density can be evaluated from the electric field in the radial direction at the boundary through the Gauss-law constraint. The quark chemical potential is thus the time component of the $U(1)$ vector potential, A_0, at the boundary, which is conjugate to the electric

field [52, 53]. This fits the conventional GKP-Witten prescription: The boundary value of A_0 gives the source (the chemical potential); the expectation value of the conjugate operator (the density) is given by the derivative of A_0 at the boundary with respect to the radial direction. These quantities are boundary conditions for the Gauss-law constraint which may be chosen arbitrarily. However, another physical condition *in the bulk*, i.e., the bulk condition, fixes the ambiguity in the relationship between them whenever the GKP-Witten prescription works. To the best of the authors' knowledge, only the example where the bulk condition is yet to be known is the finite density systems of baryons.

The origin of the ambiguity can be understood in the following way. The global $U(1)_B$ ($U(1)$-baryon) symmetry is enhanced to the $U(1)$ gauge symmetry in the gravity dual. The constant shift of the boundary value of A_0 can be a gauge transformation which does not alter the physics in the gravity dual whereas the constant shift of the chemical potential has definite physical meaning in the boundary theory. This contradiction is resolved when the flavor brane intersects the horizon: A_0 has to vanish at the horizon to make the one-form well-defined there [54, 55]. This removes the ambiguity of the constant shift of the boundary value of A_0. However, we cannot employ this prescription if the flavor brane does not intersect the horizon. One way to estimate the chemical potential may be to perform a Legendre transformation [56, 55, 57] to the canonical ensemble where the chemical potential is given by differentiating the Helmholtz free energy with respect to the charge. However, the success of the conventional GKP-Witten prescription implies the presence of an unknown bulk condition from which the baryon chemical potential at a given baryon density is uniquely assigned within the grand canonical ensemble.

More serious problem is the difficulty to incorporate many-body systems of dynamical baryons. In the phase where the flavor brane is away from the horizon, quarks are confined. The $U(1)_B$ charge is carried by baryons in this case. The baryon is holographically realized as a baryon vertex [43, 58] which consists of the fundamental strings and a D-brane wrapped on a compact subspace. In order to prepare a system of finite density of baryons, we need to deal with many-body physics of wrapped D-branes on a curved spacetime which is quite a challenge within the current technology of the superstring theory. The baryons can also be described as solitons (or Skyrmion-like objects) [38, 39, 40] on the effective worldvolume theory of the flavor brane. However, we still need to deal with many-body problems of solitons on a curved spacetime. Because of these difficulties, the baryons have been introduced as point-like objects localized at the most IR point (the most distant point from the boundary) on the flavor brane in most of the

literature. However, since the baryons are dynamical objects, their distribution along the radial direction should be determined dynamically. Thus, a gravity dual to deal with the dynamical baryons at finite density has been awaited.

Examples of the attempts to incorporate the dynamical baryons in the gravity dual are as follows. Point-like massive baryons localized at the most IR point were first introduced to the gravity dual at finite baryon density in Ref. [59]. In Ref. [60], baryon vertices attached to a flavor brane at the most IR point were introduced to a holographic dual of finite baryon density. However, singular configurations of the baryon vertices and the flavor branes have been used so far in this approach. An attempt to take account of the distribution of the baryons in the bulk has been made in Ref. [61], but the distribution of the baryons or the energy density of the system obtained there were found to be singular for the spatially homogeneous setups. Bulk baryon fields have been introduced [62, 39] to models of holographic QCD. An analysis of the baryon mass at finite baryon density was done [63] within the model of Ref. [62], but the dynamics of the $U(1)$ gauge field does not reflect the dynamics of the baryon field.

A holographic treatment of the fermion many-body system in the confinement phase is also made in terms of the Fermi liquid in $2 + 1$ dimensions [64]. There, instead of imposing suitable boundary conditions, the Fermi distribution of the boundary theory is introduced as an input to obtain the relation between the chemical potential and the charge density.

In this study, we introduce a holographic mean-field theory for fermions to describe many-body systems of dynamical fermions including baryons. In the boundary theory, the one-point expectation value of the fermionic operator has to vanish (in the absence of the conjugate fermionic source) while the bi-linear operator of the fermions, such as the density operator, can carry a non-zero expectation value: the conventional mean-field approach makes sense for the bi-linear operators, but not for the fermionic field itself. However, we point out that the things are different in the holographic dual. The expectation value of the fermionic operator is given by the boundary value of the corresponding bulk fermionic field [65]. Therefore, we can introduce a non-vanishing classical fermionic field in the bulk while maintaining the expectation value of the boundary fermionic operator to be zero. The non-vanishing bulk fermionic field induces non-zero expectation values of the bi-linear operators, such as the charge density which is detected by the derivative of the $U(1)$ gauge field. We call the non-vanishing classical fermionic field in the bulk the *holographic mean field*. The dynamical distribution of the fermions along the radial direction is realized by the dynamics of the holographic mean field.

The holographic mean field is requested to carry the $U(1)$ charge. The coupled equations of motion for the fermions and the $U(1)$ gauge field give an eigenvalue equation from which the chemical potential is unambiguously fixed. It will also be shown that the chemical potential at the zero-density limit automatically agrees with the mass of the fermion. Thus, the above mentioned problems are resolved in harmony in our approach.

5.2 The holographic mean-field theory

Let us consider a dual geometry without an event horizon whose metric of the non-compact 5d part depends only on the radial coordinate, the fifth direction. The 5d metric can be transformed to the conformally flat metric

$$ds_{5d}^2 = H(w)(dw^2 + \eta_{\mu\nu}dx^\mu dx^\nu)\,, \tag{5.1}$$

by an appropriate coordinate transformation unless the geometry has a horizon. Here, $\eta_{\mu\nu}$ is diag$(-,+,+,+)$. We consider the dimensionally-reduced theory on the 5d geometry (5.1) assuming that all the bulk fields depend only on $(w,\ x^\nu)$. We introduce a Dirac spinor Ψ on the 5d geometry which interacts with a bulk $U(1)$ gauge field A_M. The actions for Ψ and A_M are

$$\begin{aligned} S_\Psi &= \int d^4x dw \left[i\bar{\Psi}\Gamma^M(\partial_M - iqA_M)\Psi - m_5(w)\bar{\Psi}\Psi \right], \\ S_A &= \int d^4x dw \mathcal{L}_A\,, \end{aligned} \tag{5.2}$$

where q and $m_5(w)$ denote the charge and the 5d mass of the fermion, respectively. The vielbein and the spin connection are absorbed by a suitable field redefinition of the fermion field. The possible boundary terms and the counter terms are omitted here. The w dependence of $m_5(w)$ reflects the curvature of the original geometry. Γ^M are written in terms of the 4d Dirac matrices as $\Gamma^\nu = \gamma^\nu$ $(\nu = 0,1,2,3)$ and $i\Gamma^w = \gamma^5$. We employ the probe approximation such that the fermion field and the gauge field do not modify the geometry: we regard $S = S_\Psi + S_A$ as the total action up to the action of the gravity sector.

We work in the $A_w(x,w) = 0$ gauge, and replace the gauge field with the mean field as

$$A_0(x,w) \to A_0(w)\,, \quad A_i(x,w) \to A_i(w)\,, \tag{5.3}$$

where $i = (1, 2, 3)$. We identify

$$A_0(w)\Big|_{\text{boundary}} = \mu\,, \quad A_i(w)\Big|_{\text{boundary}} = 0 \tag{5.4}$$

where μ is the chemical potential associated with the fermion charge. We now explain how we formulate the holographic mean-field approach for the fermion field. We introduce the holographic mean field as

$$\Psi(x, w) \to \Psi(w)\,. \tag{5.5}$$

The non-vanishing mean field realizes the dynamical distribution of the charge in w direction, which is given by

$$\rho(w) = q\Psi^\dagger(w)\Psi(w)\,. \tag{5.6}$$

The integration over w gives the 4d charge density n. In the present analysis, we switch off the fermionic source. The one-point expectation value of the fermionic field of the boundary theory has to vanish in the absence of the fermionic source, then

$$\Psi(w)\Big|_{\text{boundary}} = 0\,. \tag{5.7}$$

We also require that the mean fields are regular.

Now $A_0' \equiv \partial_w A_0$ is given by the Gauss-law constraint:

$$\partial_w \frac{\partial \mathcal{L}_{\text{A}}}{\partial A_0'(w)} - q\Psi^\dagger(w)\Psi(w) = 0\,, \tag{5.8}$$

while $A_i' \equiv \partial_w A_i$ is given by

$$\partial_w \frac{\partial \mathcal{L}_{\text{A}}}{\partial A_i'(w)} - q\Psi^\dagger(w)\Gamma^0\Gamma^i\Psi(w) = 0\,. \tag{5.9}$$

The scalar potential $A_0(w)$ is given by using $A_0'(w)$:

$$A_0(w) = \mu + \int_{\text{boundary}}^{w} dw' A_0'(w') \equiv \mu + \tilde{A}_0(w)\,. \tag{5.10}$$

However, the boundary value μ is arbitrary at this stage. In other words, whatever value of μ can give the same charge distribution. This has been a problem in holographic models at finite density. This problem will be resolved by solving the equation of motion for $\Psi(w)$:

$$\left[i\Gamma^w\partial_w + q\Gamma^0 A_0(w) + q\Gamma^i A_i(w) - m_5(w)\right]\Psi(w) = 0\,, \tag{5.11}$$

where the mean field $\Psi(w)$ and hence the charge distribution depend on the boundary value of $A_0(w)$.

Let us see how it works explicitly. We write $\Psi(w)$ in terms of the two-component spinors $\Psi_\pm$ as

$$\Psi(w) = \begin{pmatrix} \Psi_+ \\ \Psi_- \end{pmatrix}, \tag{5.12}$$

with the Dirac matrices given by

$$i\Gamma^w = \begin{pmatrix} 0 & 1 \\ 1 & 0 \end{pmatrix}, \Gamma^0 = \begin{pmatrix} 1 & 0 \\ 0 & -1 \end{pmatrix}, \Gamma^i = \begin{pmatrix} 0 & \sigma^i \\ -\sigma^i & 0 \end{pmatrix}. \tag{5.13}$$

We assume rotational invariance in 3d space, thus we can take $A_1(w) = A_2(w) = 0$, and hence $\sigma^3\Psi_\pm = \Psi_\pm$ without loss of generality. From (5.11), we obtain

$$\begin{aligned} &[\partial_w - qA_3(w)]\Psi_+ - [m_5(w) + q\tilde{A}_0(w)]\Psi_- = q\mu\Psi_-\,, \\ &[\partial_w + qA_3(w)]\Psi_- - [m_5(w) - q\tilde{A}_0(w)]\Psi_+ = -q\mu\Psi_+\,. \end{aligned} \tag{5.14}$$

Solving (5.14) coupled with (5.8) and (5.9), $q\mu$ is obtained as the eigenvalue for a given value of $n = \int dw\, q\Psi^\dagger(w)\Psi(w)$. Note that n determines the normalization of $\Psi(w)$ as well. In this way, the holographic mean-field theory provides the equation of state (EOS): the relation between the 4d charge density n and the chemical potential μ is determined dynamically. The new bulk condition to fix the ambiguity of μ in the GKP-Witten prescription is the regularity of the fermionic mean field under (5.7).

In order to obtain the energy spectrum of the quasifermions for given n, we need to introduce the fluctuations $\psi(x,w), a_\nu(x,w)$ on top of the mean fields $\Psi(w), A_\nu(w)$ as

$$\begin{aligned} \Psi(x,w) &= \Psi(w) + \psi(x,w)\,, \\ A_\nu(x,w) &= A_\nu(w) + a_\nu(x,w)\,. \end{aligned} \tag{5.15}$$

The 4d Fourier-transformed fluctuations obey

$$\begin{aligned} &[i\Gamma^w\partial_w + \Gamma^0(p_0 + qA_0(w)) + \Gamma^3 qA_3(w) + \vec{\Gamma}\cdot\vec{p} - m_5(w)]\psi(p_0,\vec{p},w) \\ &+ \Psi(w)\Gamma^\nu q a_\nu(p_0,\vec{p},w) = 0\,, \end{aligned} \tag{5.16}$$

where the mean fields $A_0(w), A_3(w)$ are already determined above. By solving (5.16) coupled with the equation of motion for a_ν for given momentum $\vec{p}$, we obtain the energy eigenvalue $p_0 + q\mu$ and thus the dispersion relation.

Let us discuss the zero density limit, $n \to 0$. (5.8) and (5.9) tell us that $\tilde{A}_0(w) \to 0, A_3(w) \to 0$, and (5.14) becomes

$$\begin{aligned} \partial_w \Psi_+ - m_5(w)\Psi_- &= q\mu\Psi_- , \\ \partial_w \Psi_- - m_5(w)\Psi_+ &= -q\mu\Psi_+ . \end{aligned} \tag{5.17}$$

On the other hand, at $\mu = 0$, (5.16) is reduced to be

$$\begin{aligned} \partial_w \psi_+ - m_5(w)\psi_- &= m_f\psi_- , \\ \partial_w \psi_- - m_5(w)\psi_+ &= -m_f\psi_+ , \end{aligned} \tag{5.18}$$

where $\psi = (\psi_+, \psi_-)^T$ and we used $\Gamma^\nu p_\nu \psi = m_f \psi$.

The lowest eigenvalue m_f of (5.18) for the non-vanishing eigenfunction under the boundary condition $\psi\big|_{\text{boundary}} = 0$ is the mass of the fermion in the ground state. Therefore, the chemical potential determined by (5.17) for the non-vanishing density coincides with the fermion mass, i.e., $q\mu \to m_f$ at the limit $n \to 0$. We do not find any nontrivial solutions for $\Psi(w)$ for $|q\mu| < m_f$, where there is no formation of the Fermi surface. The chemical potential μ_{on} for onset of the density automatically agrees with the fermion mass in our approach as a consequence of the dynamics. If we know m_f *a priori*, the condition $q\mu_{\text{on}} = m_f$ may be used to fix the constant shift of A_0, but this does not necessarily fix the gauge at arbitrary density.

5.3 The equation of state for baryon many-body systems

Now we demonstrate how to obtain the EOS for baryon many-body systems. We apply our method to the model [39] dealing with the fluctuation of the baryon field at $\mu = 0$. The boundaries in this model are located at $w = \pm w_{\text{max}}$, thus the boundary conditions for the mean fields are $A_0(\pm w_{\text{max}}) = \mu$, $A_3(\pm w_{\text{max}}) = 0$, $\Psi(\pm w_{\text{max}}) = 0$. Here μ denotes the baryon chemical potential and then $q = 1$. We assume that the theory is invariant under the 5d parity $(t, \mathbf{x}, w) \to (t, -\mathbf{x}, -w)$. Therefore, $A_0(w)$ ($A_3(w)$) is an even (odd) function of w, and the regularity condition leads to $A_0'(0) = 0$ ($A_3(0) = 0$). From the parity invariance, $\Psi_+(w)$ is either an even function of w or an odd function. The former implies that $\Psi_+(w)$ is the mean field for the even parity baryons, and the latter for the odd parity baryons. Here we consider the distribution of the even parity baryons, and the regularity condition requires $\Psi_+'(0) = 0$.

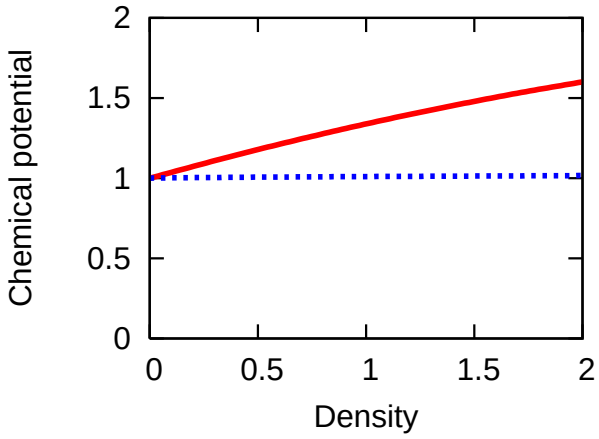

Figure 5.1: The EOS of the model (solid) compared with the one for the free baryons (dashed): $\mu/\mu_{n\to 0} = \sqrt{1 + (3\pi^2 n/2)^{2/3}/\mu_{n\to 0}^2}$. The horizontal axis is n/n_0, while the vertical axis is $\mu/\mu_{n\to 0}$.

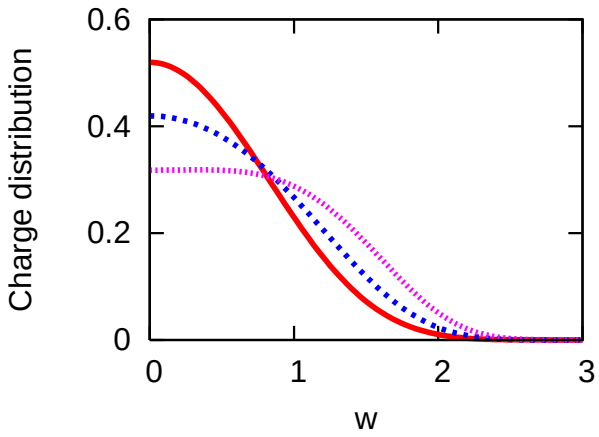

Figure 5.2: The baryon charge distribution $\rho(w)/n$ for $n/n_0 = 0.1$ (solid), 1 (dashed) and 2 (dotted). The boundary is located at $w = w_{\max} \simeq 3.64$.

We use the DBI action of the D8-branes as S_A:

$$S_A = -C \int d^4x dw U^{1/4}(w) \sqrt{H^3(w)\{H^2(w) - (2\pi l_s^2/N_c)^2[(A_0'(w))^2 - (A_3'(w))^2]\}}\,, \tag{5.19}$$

where $C = (2\pi)^{-7}(4\pi^2/3) l_s^{-11/2} \lambda^{1/4} (2M_{\rm KK})^{-1/4} N_f N_c$, and the $A_0(w)$ here is N_c times $A_0(w)$ in the standard convention. Here, $M_{\rm KK}$ is the energy scale of the theory, λ is the 't Hooft coupling, N_c is the number of colors, N_f is the number of flavors, and l_s is the string length which does not show up in the end of the calculation. The definitions of $U(w)$ and $H(w)$ are given in [39].

We fix $M_{\rm KK}$ and λ in the same way as in [14]: $M_{\rm KK} = 949\,\text{MeV}$ and $\lambda N_c = 50$. We consider $N_f = 2$ case, and use the normal nuclear matter density $n_0 = 0.16\,\text{fm}^{-3}$ to scale the baryon number density n. Figure 5.1 shows the resultant EOS compared with the one for the free baryons. The chemical potential μ increases as the density grows. The increase of μ is quite larger than that of the free baryons, which indicates that the interactions among the baryons are taken into account.

Figure 5.2 shows the density dependence of the baryon charge distribution $\rho(w)$, which is indeed regular. The distribution shifts to the boundary side as the density grows. This implies that taking account of the distribution of the baryon charge along the radial direction becomes important at the high density regions.

5.4 Discussions

We have proposed a holographic mean-field theory to analyze many-body systems of fermions. We have seen that our approach provides the relation between the charge density and the chemical potential, the equation of state. We have applied this method to the HRYY model and have presented the equation of state for baryon many-body systems. In this way, we obtain a way for analyzing holographic models in which the dynamics of the baryons and that of the $U(1)_B$ gauge fields in the bulk are inclusively considered.

We expect that our approach is applicable to various physical subjects related to dense matter. Investigating the density dependence of the masses/dispersion relations and the decay constants of hadrons and the couplings among them must be interesting. When we discuss the stability of neutron stars, it is important to obtain the equation of state for the nuclear matter, and our approach can help it.

Of course, improving our approach to obtain a more sophisticated model is also valuable. One direction is to include anti-fermion degrees of freedom which

is neglected in our approach. Another direction is to take into account the back-reaction of the matter to spacetime geometry which becomes important at high density regions.

Chapter 6

Summary

We have presented our studies about QCD at finite density using effective models.

In Chapter 2, we have explored general features of thermodynamic quantities and hadron mass spectra in a possible phase where chiral $SU(2)_L \times SU(2)_R$ symmetry is spontaneously broken while its center Z_2 symmetry remains. In this phase, chiral symmetry breaking is driven by a quartic quark condensate rather than a bilinear quark condensate which is possible at finite density. A Ginzburg-Landau study leads to a new tricritical point between the Z_2 broken and unbroken phases. The quark number density exhibits an abrupt change near the restoration of the center symmetry rather than that of the chiral symmetry. Hadron masses in possible phases are also studied in a linear sigma model. We have shown that, in the Z_2 symmetric phase, the Nambu-Goldstone boson is a pure four-quark state, and the masses of the nucleon in the excited state and its parity partner are degenerated.

In Chapter 3, we have reviewed previous studies about holographic models of QCD. We have shown how the mass and the decay constants are calculated in the hard-wall model. Then we have shown the construction of the Sakai-Sugimoto model. We have also mentioned some attempts to introduce baryons into the Sakai-Sigimoto model.

In Chapter 4, we have investigate the $\rho - a_1$ mixing in dense baryonic matter by using a holographic model in the bottom-up approach. We have used a 5d geometry such that the backreaction of the matter to spacetime geometry is taken into account. In the model, the 5d Chern-Simons term causes a mixing between the ρ and a_1 mesons at finite density and at finite momentum. We have shown that the mixing between ρ and a_1 becomes stronger due to the backreaction of the mater to the spacetime geometry. The holographic model we have used here

is though, does not include dynamical baryons despite we consider the system in dense baryonic matter. This gives us a strong motivation to obtain the holographic model at finite density including dynamical baryons.

In Chapter 5, we have proposed the holographic mean-field theory to analyze many-body systems of fermions including baryons. We have applied our approach to the HRYY model to obtain the holographic model for finite-density systems of baryons, and have presented the equation of state for the system.

We think that our studies surely made some contributions to get a better understanding about QCD at finite density, but at the same time, we feel that we still have a long way to go. We hope QCD will continuously provide many interesting topics to study and keep us enjoyed and annoyed.

Acknowledgments

I am deeply grateful to my adviser, Professor Masayasu Harada for introducing me to the research field of QCD and giving many opportunities to enjoy researches. During my student life in his group for 6 years, I had a opportunity to tackle 5 research topics: Critical phenomena around the QCD critical point, Ginzburg-Landau study of the phase diagram including the phase with unbroken center symmetry, Non-local NJL model study of the phase with unbroken center symmetry, $\rho - a_1$ mixing in holographic QCD, and Holographic mean-field theory. He always gave me fruitful suggestions. I would like to thank my collaborators, Professor Chihiro Sasaki and Professor Shin Nakamura. Discussions with them was very exciting, illuminating and helpful. I appreciate Professor Youngman Kim for giving me a chance to stay and study in his group in APCTP. I really enjoyed the research, the seminars and the life in APCTP. I really thank Professor Chiho Nonaka in our group for always telling me about fresh topics in heavy-ion collision physics.

I am thankful to all the members of H-lab, E-lab, and Q-lab. Without their support, I would not be able to accomplish this thesis.

My work has been supported in part by Global COE Program "Quest for Fundamental Principles in the Universe" of Nagoya University (G07).

Appendix A

Phase boundaries from Ginzburg-Landau potential

The relevant expressions for the phase boundaries obtained from the potential (2.10) are given below. We will take $D = F = 0$ and the chiral limit $h = 0$.

- Second-order phase transition when $B \geq 1/4$:

$$A = 0\,. \tag{.1}$$

  The solutions for σ and χ on this boundary are given by

$$(\sigma_0\,, \chi_0) = (0\,, 0)\,. \tag{.2}$$

- First-order phase transition when $0 \leq B < 1/4$ and $0 < A \leq 1/8$:

$$A = \left(\frac{3}{8} - \sqrt{\left(\frac{3}{8}\right)^2 + \frac{1}{2}\left(B - \frac{1}{4}\right)}\right)\sqrt{-\frac{3}{8} - 2\left(B - \frac{1}{4}\right) + \sqrt{\left(\frac{3}{8}\right)^2 + \frac{1}{2}\left(B - \frac{1}{4}\right)}}\,. \tag{.3}$$

The solutions for σ and χ on this boundary are given by

$$(\sigma_0, \chi_0) = (0, 0),$$

$$\left(\pm \left[\frac{1}{2} \left(\frac{1}{8} + \sqrt{\left(\frac{3}{8}\right)^2 + \frac{1}{2}\left(B - \frac{1}{4}\right)} \right) \sqrt{-\frac{3}{8} - 2\left(B - \frac{1}{4}\right) + \sqrt{\left(\frac{3}{8}\right)^2 + \frac{1}{2}\left(B - \frac{1}{4}\right)}} \right]^{1/2}, \right.$$

$$\left. \frac{1}{2} \sqrt{-\frac{3}{8} - 2\left(B - \frac{1}{4}\right) + \sqrt{\left(\frac{3}{8}\right)^2 + \frac{1}{2}\left(B - \frac{1}{4}\right)}} \right). \qquad (.4)$$

- First-order phase transition when $-1/8 < B < 0$ and $1/8 < A < 1/4$:

$$A = \frac{1}{8} - B. \qquad (.5)$$

The solutions for σ and χ on this boundary are given by

$$(\sigma_0, \chi_0) = \left(0, \pm\sqrt{\frac{-B}{2}}\right), \quad \left(\pm\sqrt{\frac{1}{2}\left(B + \frac{1}{8}\right)}, \frac{1}{4}\right). \qquad (.6)$$

- Second-order phase transition when $B \leq -1/8$ and $A \geq 1/4$:

$$A = \sqrt{-\frac{B}{2}}. \qquad (.7)$$

The solutions for σ and χ on this boundary are given by

$$(\sigma_0, \chi_0) = \left(0, \pm\sqrt{\frac{-B}{2}}\right). \qquad (.8)$$

- Second-order phase transition when $A > 1/8$:

$$B = 0. \qquad (.9)$$

The solutions for σ and χ on this boundary are given by

$$(\sigma_0, \chi_0) = (0, 0). \qquad (.10)$$

Bibliography

[1] For a recent review, see e.g., C. Hoelbling, PoSLATTICE **2010**, 011 (2010) [arXiv:1102.0410 [hep-lat]].

[2] N. Ishii, S. Aoki and T. Hatsuda, Phys. Rev. Lett. **99**, 022001 (2007) [nucl-th/0611096].

[3] For a recent review, see e.g., K. Kanaya, PoSLATTICE **2010**, 012 (2010).

[4] For a recent review, see e.g., S. Muroya, A. Nakamura, C. Nonaka and T. Takaishi, Prog. Theor. Phys. **110**, 615 (2003).

[5] For a recent review, see e.g., S. Gupta, PoSLATTICE **2010**, 007 (2010).

[6] D. Bailin and A. Love, Phys. Rept. **107**, 325 (1984);
M. G. Alford, K. Rajagopal and F. Wilczek, Phys. Lett. B **422**, 247 (1998);
M. G. Alford, K. Rajagopal and F. Wilczek, Nucl. Phys. B **537**, 443 (1999).

[7] D. Blaschke, H. Grigorian and D. N. Voskresensky, Astron. Astrophys. **424**, 979 (2004);

[8] M. G. Alford, J. A. Bowers and K. Rajagopal, J. Phys. GG **27**, 541 (2001) [Lect. Notes Phys. **578**, 235 (2001)].

[9] G. E. Brown and M. Rho, Phys. Rev. Lett. **66**, 2720 (1991);
T. Hatsuda and S. H. Lee, Phys. Rev. C **46**, 34 (1992).

[10] R. Rapp and J. Wambach, Adv. Nucl. Phys. **25**, 1 (2000);
R. S. Hayano and T. Hatsuda, Rev. Mod. Phys. **82**, 2949 (2010);
R. Rapp, J. Wambach and H. van Hees, arXiv:0901.3289 [hep-ph].

[11] J. M. Maldacena, Adv. Theor. Math. Phys. **2**, 231 (1998) [Int. J. Theor. Phys. **38**, 1113 (1999)]

[12] S. S. Gubser, I. R. Klebanov and A. M. Polyakov, Phys. Lett. B **428**, 105 (1998) [arXiv:hep-th/9802109].

[13] E. Witten, Adv. Theor. Math. Phys. **2**, 253 (1998) [arXiv:hep-th/9802150].

[14] T. Sakai, S. Sugimoto, Prog. Theor. Phys. **113**, 843-882 (2005).

[15] J. Erlich, E. Katz, D. T. Son, M. A. Stephanov, Phys. Rev. Lett. **95**, 261602 (2005).

[16] M. Harada, C. Sasaki, S. Takemoto, Phys. Rev. **D81**, 016009 (2010).

[17] M. Knecht and J. Stern, arXiv:hep-ph/9411253, J. Stern, arXiv:hep-ph/9712438, arXiv:hep-ph/9801282.

[18] B. Holdom and G. Triantaphyllou, Phys. Rev. D **51**, 7124 (1995);
Phys. Rev. D **53**, 967 (1996);
B. Holdom, Phys. Rev. D **54**, 1068 (1996).

[19] P. Maris and Q. Wang, Phys. Rev. D **53**, 4650 (1996);
F. S. Roux, T. Torma and B. Holdom, Phys. Rev. D **61**, 056009 (2000).

[20] I. I. Kogan, A. Kovner and M. A. Shifman, Phys. Rev. D **59**, 016001 (1999).

[21] Y. Watanabe, K. Fukushima and T. Hatsuda, Prog. Theor. Phys. **111**, 967 (2004).

[22] A. Armoni, A. Gorsky and M. Shifman, Phys. Rev. D **72**, 105001 (2005).

[23] B. Y. Park, D. P. Min, M. Rho and V. Vento, Nucl. Phys. A **707**, 381 (2002);
H. J. Lee, B. Y. Park, D. P. Min, M. Rho and V. Vento, Nucl. Phys. A **723**, 427 (2003);
M. Rho, arXiv:0711.3895 [nucl-th].

[24] L. McLerran and R. D. Pisarski, Nucl. Phys. A **796**, 83 (2007);
Y. Hidaka, L. D. McLerran and R. D. Pisarski, Nucl. Phys. A **808**, 117 (2008).

[25] L. McLerran, K. Redlich and C. Sasaki, Nucl. Phys. A **824**, 86 (2009).

[26] A. Heinz, S. Struber, F. Giacosa and D. H. Rischke, Phys. Rev. D **79**, 037502 (2009).

[27] C. Sasaki, B. Friman and K. Redlich, Phys. Rev. D **75**, 074013 (2007).

[28] H. Fujii and M. Ohtani, Phys. Rev. D **70**, 014016 (2004).

[29] M. Kitazawa, T. Koide, T. Kunihiro and Y. Nemoto, Prog. Theor. Phys. **108**, 929 (2002).

[30] T. Hatsuda, M. Tachibana, N. Yamamoto and G. Baym, Phys. Rev. Lett. **97**, 122001 (2006);

N. Yamamoto, M. Tachibana, T. Hatsuda and G. Baym, Phys. Rev. D **76**, 074001 (2007).

[31] T. Schafer and F. Wilczek, Phys. Rev. Lett. **82**, 3956 (1999).

[32] M. Asakawa and K. Yazaki, Nucl. Phys. A **504**, 668 (1989);

J. Berges and K. Rajagopal, Nucl. Phys. B **538**, 215 (1999);

A. M. Halasz, A. D. Jackson, R. E. Shrock, M. A. Stephanov and J. J. M. Verbaarschot, Phys. Rev. D **58**, 096007 (1998);

Y. Hatta and T. Ikeda, Phys. Rev. D **67**, 014028 (2003).

[33] C. E. Detar and T. Kunihiro, Phys. Rev. D **39**, 2805 (1989);

Y. Nemoto, D. Jido, M. Oka and A. Hosaka, Phys. Rev. D **57**, 4124 (1998);

D. Jido, Y. Nemoto, M. Oka and A. Hosaka, Nucl. Phys. A **671**, 471 (2000);

H. c. Kim, D. Jido and M. Oka, Nucl. Phys. A **640**, 77 (1998);

D. Jido, T. Hatsuda and T. Kunihiro, Phys. Rev. Lett. **84**, 3252 (2000);

S. Gallas, F. Giacosa and D. H. Rischke, arXiv:0907.5084 [hep-ph].

[34] R. D. Pisarski and F. Wilczek Phys. Rev. D **29**, 338 (1984).

[35] T. D. Cohen and W. Broniowski, Phys. Lett. B **342**, 25 (1995).

[36] K . Nakamura et al. (Particle Data Group), J. Phys. G **37**, 075021 (2010).

[37] E. Witten, Adv. Theor. Math. Phys. **2**, 505 (1998) [hep-th/9803131].

[38] K. Nawa, H. Suganuma and T. Kojo, Phys. Rev. D **75**, 086003 (2007).

[39] D. K. Hong, M. Rho, H. U. Yee and P. Yi, Phys. Rev. D **76**, 061901 (2007); JHEP **0709**, 063 (2007).

[40] H. Hata, T. Sakai, S. Sugimoto and S. Yamato, Prog. Theor. Phys. **117**, 1157 (2007).

[41] K. Hashimoto, T. Sakai and S. Sugimoto, Prog. Theor. Phys. **120**, 1093 (2008).

[42] K. Hashimoto, T. Sakai and S. Sugimoto, Prog. Theor. Phys. **122**, 427 (2009).

[43] D. J. Gross and H. Ooguri, Phys. Rev. D **58**, 106002 (1998).

[44] E. Witten, JHEP **9807**, 006 (1998).

[45] G. S. Adkins, C. R. Nappi and E. Witten, Nucl. Phys. B **228**, 552 (1983).

[46] S. K. Domokos, J. A. Harvey, Phys. Rev. Lett. **99**, 141602 (2007).

[47] M. Harada, C. Sasaki, Phys. Rev. **C80**, 054912 (2009).

[48] B. -H. Lee, C. Park, S. -J. Sin, JHEP **0907**, 087 (2009);
K. Jo, B. -H. Lee, C. Park, S. -J. Sin, JHEP **1006**, 022 (2010).

[49] S. Nakamura, H. Ooguri and C. S. Park, Phys. Rev. D **81**, 044018 (2010).

[50] M. Harada, S. Nakamura and S. Takemoto, arXiv:1112.2114 [hep-th].

[51] A review on the holographic description of quark/flavor sectors is, for example, J. Erdmenger, N. Evans, I. Kirsch and E. Threlfall, Eur. Phys. J. A **35**, 81 (2008).

[52] K. Y. Kim, S. J. Sin and I. Zahed, arXiv:hep-th/0608046.

[53] N. Horigome and Y. Tanii, JHEP **0701**, 072 (2007).

[54] H. W. Braden, J. D. Brown, B. F. Whiting and J. W. York Jr., Phys. Rev. D **42**, 3376 (1990).

[55] S. Kobayashi, D. Mateos, S. Matsuura, R. C. Myers and R. M. Thomson, JHEP **0702**, 016 (2007).

[56] S. Nakamura, Y. Seo, S. J. Sin and K. P. Yogendran, J. Korean Phys. Soc. **52**, 1734 (2008);

S. Nakamura, Y. Seo, S. J. Sin and K. P. Yogendran, Prog. Theor. Phys. **120**, 51 (2008).

[57] S. Nakamura, Prog. Theor. Phys. **119**, 839 (2008).

[58] E. Witten, JHEP **9807**, 006 (1998).

[59] O. Bergman, G. Lifschytz and M. Lippert, JHEP **0711**, 056 (2007).

[60] Y. Seo and S. J. Sin, JHEP **0804**, 010 (2008).

[61] M. Rozali, H. H. Shieh, M. Van Raamsdonk and J. Wu, JHEP **0801**, 053 (2008).

[62] D. K. Hong, T. Inami and H. -U. Yee, Phys. Lett. B **646**, 165 (2007).

[63] Y. Kim, C. H. Lee and H. U. Yee, Phys. Rev. D **77**, 085030 (2008);

K. Kim, S. H. Lee and Y. Kim, talk given at HNP09 (2009), http://www.rcnp.osaka-u.ac.jp/ hnp09/slide/nov18/k.kim.pdf.

[64] S. Sachdev, Phys. Rev. D **84**, 066009 (2011).

[65] M. Henningson and K. Sfetsos, Phys. Lett. B **431**, 63 (1998); M. Henneaux, arXiv:hep-th/9902137.

副論文１

Enhancement of quark number susceptibility with an alternative pattern of chiral symmetry breaking in dense matter

（有限密度中におけるカイラル対称性の破れに伴うクォーク数感受率の増大）

Masayasu Harada, Chihiro Sasaki, and Shinpei Takemoto

Physical Review D81, 016009 (2010)

副論文 2

Holographic mean-field theory for baryon many-body systems
（ホログラフィック平均場理論をもちいたバリオン多体系の解析）

Masayasu Harada, Shin Nakamura and Shinpei Takemoto

arXiv:1112.2114 [hep-th]